1971

Mathematical simulation of the solidification of steel in the electroslag remelting process

Jean-Louis Galzin
Lehigh University

MATHEMATICAL SIMULATION OF THE SOLIDIFICATION OF STEEL IN THE ELECTROSLAG REMELTING PROCESS

Jean-Louis Galzin

ABSTRACT

A mathematical model of the solidification process in an ingot remelted by the continuous electroslag process was developed to predict the influence of process parameters on the temperature distribution of the ingot and more precisely on the shape of the molten metal pool. The model essentially consists of a computer program which was written for a two and three dimensional analysis of the problem. The three dimensional model results in a very good prediction of the depth and shape of the pool for the range of melting rates studied. The computer model proposed is a three dimensional heat transfer program which can be generalized easily to a variety of shapes and boundary conditions.

MATHEMATICAL SIMULATION OF THE SOLIDIFICATION OF STEEL IN THE ELECTROSLAG REMELTING PROCESS

by

Jean-Louis Galzin

A Thesis

Presented to the Graduate Committee

of Lehigh University

in Candidacy for the Degree of

Master of Science

in

Metallurgy and Materials Science

Lehigh University

1971

This Thesis is accepted and approved in partial fulfillment of the requirements for the degree of Master of Science.

5 March 1971
Date

Walter Charles Hahn, Jr.
Professor in Charge

G. P. Conrad III
Head of the Department

ACKNOWLEDGEMENTS

Gratitude is expressed to Dr. Walter C. Hahn for his advice and encouragement throughout this investigation and to Robert C. Parsons, of ARCOS Corporation, for his technical advice on the electroslag remelting process and his help during the experimental part of this work.

The author is also grateful to the Lehigh Chemical-Metallurgy Program for the financial support of this work.

TABLE OF CONTENTS

TABLE OF CONTENTS

LIST OF FIGURES

LIST OF FIGURES (CONTINUED)

LIST OF FIGURES (CONTINUED)

ABSTRACT

A mathematical model of the solidification process in an ingot remelted by the continuous electroslag process was developed to predict the influence of process parameters on the temperature distribution of the ingot and more precisely on the shape of the molten metal pool. The model essentially consists of a computer program which was written for a two and three dimensional analysis of the problem. The three dimensional model results in a very good prediction of the depth and shape of the pool for the range of melting rates studied. The computer model proposed is a three dimensional heat transfer program which can be generalized easily to a variety of shapes and boundary conditions.

INTRODUCTION

Modern technology has an increasing need for highly alloyed materials of high quality; more severe performance standards are required for structure and chemical composition.

In the past decade, a new interest has therefore been given to the refining processes and manufacturing procedures producing special alloys of high performance.

Among the properties required for a high quality ingot are proper chemical composition, low macro and microsegregation, absence of large non-metallic inclusions, high density and a homogeneous solidification pattern. If the ingot is to be rolled or forged, the solidification pattern is very important since the solidification process is in fact responsible for many micro and macro defects: The structure produced immediately upon solidification determines, in large measure, the properties of the part. As Winegard(1) points out, this is true also for ingots, despite the popular but incorrect belief that defects are eliminated when the ingot is forged.

In recent years, the electroslag remelting process has been regarded with special interest in this situation because of the high yield and quality of the remelted product.

FUNDAMENTALS OF THE PROCESS

As shown in Figure 1, the continuous electroslag remelting process consists of a consumable electrode which is continuously fed into a slag pool and melts because of the Joule heating at the electrode-slag interface. The droplets of liquid metal then flow down through the flux where chemical refining and mechanical removal of inclusions occur.

The refined ingot then solidifies in the lower part of the mold and is continuously withdrawn from the mold.

The characteristic features of the remelted product are its cleanliness, high density, chemical homogeneity, and absence of shrinkage flaws. The fact that the process offers a good control of micro and macro segregation of grain shape and size, and the almost axial

Figure 1

Schematic representation of the continuous electroslag process (ARCOS process).

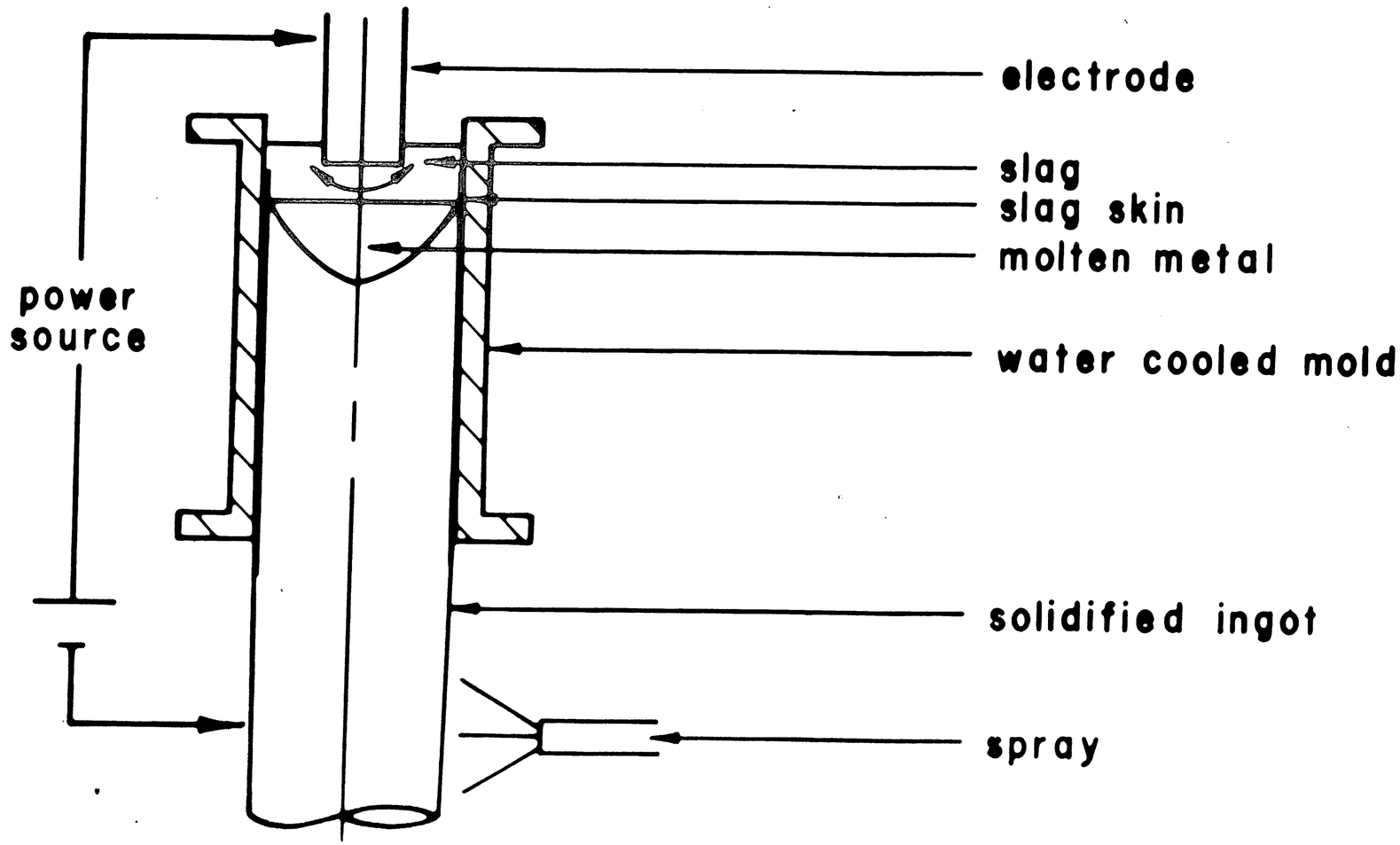
electrode
slag
slag skin
molten metal
water cooled mold
power source
solidified ingot
spray

dendritic growth is due primarily to the shallow molten metal pool. Figures 2a and 2b show the shape of the metal pool and the resulting solidification pattern in a 4 x 4 inch ingot.

However, the depth and shape of the molten metal pool are determined by the choice of operating conditions (cooling rate, melting rate, power input, slag depth) and by the grade of steel remelted.

Usually the choice of operating conditions is dictated by an empirical compromise between the need for a high melt rate (high power) for economic considerations, which may tend to give a deep metal pool, and the need for a shallow metal pool for optimum metallurgical considerations.

The control of the shape of the pool is therefore an important problem to which a rational answer must be given for future development and improvement of the process.

NEED FOR A MATHEMATICAL MODEL

The relatively large number of variables involved in the process and the great difficulty of getting accurate measurements of the pool shape during production make direct experimentation costly and only valid for the grade of steel remelted.

A mathematical model of the heat transfer process would be a highly versatile tool to simulate the solidification of an ingot; since, once the model is developed, it can be used for any set of operating conditions. Several mathematical studies of related problems have already been published(2,3,4). The case of the continuous casting of slabs has received particular interest in recent years and several models have been proposed which seem to agree well with experimental results. Unfortunately, these models are not applicable in the case of the electroslag remelting process. The main reason is that, although there is no difference in principle between the heat transfer process in a continuous casting and a continuous ESR process, some important assumptions valid for a continuous casting machine are totally incorrect in the case of the electroslag process.

Figure 2

Solidification pattern in electroslag remelted ingot.

2.a

Melting rate: 2.2 Lb/mn

2.b

Melting rate: 1.7 Lb/mn

The assumption cannot be made, for example, that the heat transfer in the direction of casting is negligible: Figure 3a represents the so-called Chalmers interface and is obtained by considering the heat flow in a semi-infinite slab, in which the thickness of the solidified shell is proportional to the square root of time. As has been proved by the experiments described in section III, the shape of the metal pool in the electrolag process is much shallower. Depending on the melting rate and cooling conditions in the mold, a shape similar to Figure 3b or 3c can be obtained. This comes from the fact that heat flow in the longitudinal direction must also be present.

A model taking this into account has recently been published by R. C. Sun(5). This model predicts the molten metal pool shape during the solidification of round ingots remelted by classical electroslag remelting (fixed bottom chilled mold).

Although there is no difference in principle between this type of process and the continuous ESR process considered in this investigation, it is believed that the possibility of spraying the ingot below the mold is an additional parameter which might have an influence on the pool shape. Furthermore, the interest of rectangular ingots is considerable for products which are later to be rolled.

It is therefore the purpose of this investigation to build a model of the solidification of a rectangular slab and predict the influence of experimental variables on the shape of the metal pool, both for steady state and dynamic conditions.

Figure 3

Compared growth of dendrites in a continuously cast ingot.

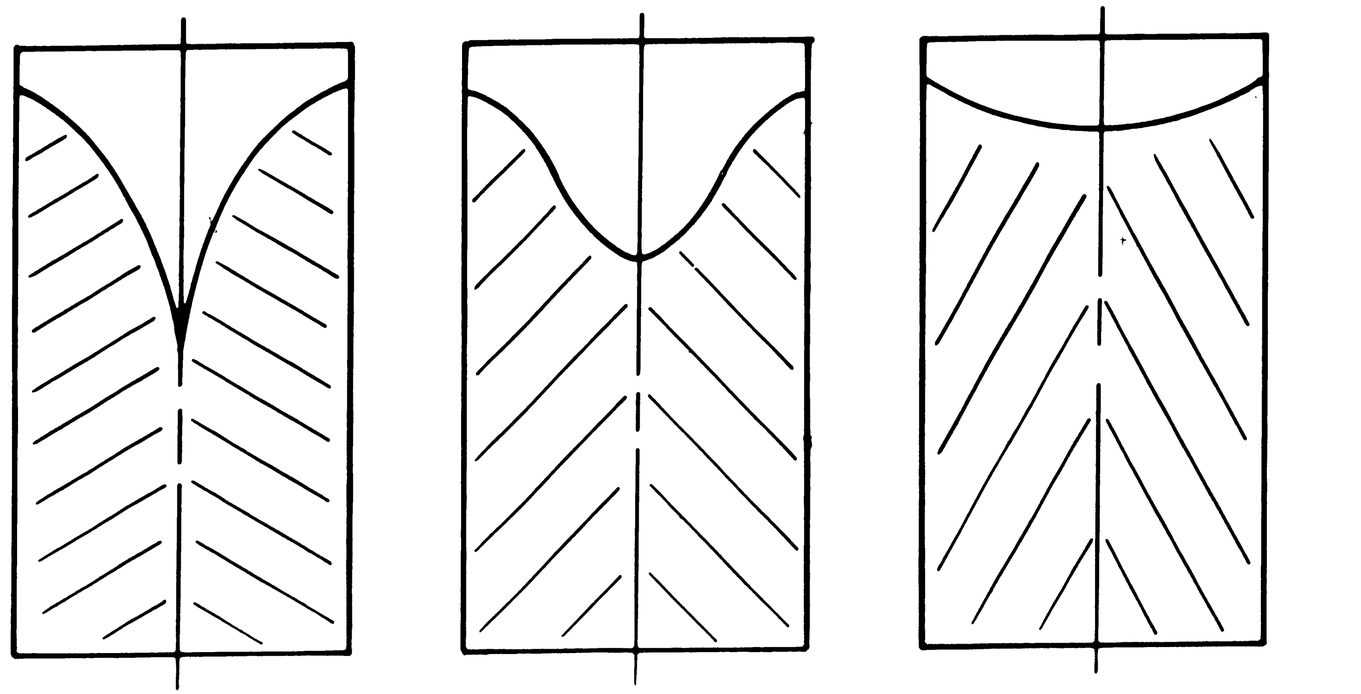

high extraction rate

low extraction rate

very low extraction rate

MODEL APPROACH

As has already been pointed out, several analytical treatments of related problems have been proposed(6,7,8). But both the simplifying assumptions in these models and the complexity of the analytical solutions are serious disadvantages. Numerical solutions, which are considerably more versatile, appear to be better suited.

FINITE DIFFERENCE SOLUTIONS OF THE HEAT EQUATION

The principle of the finite difference method is to replace the continuous region in which the solution is sought by a finite number of mesh points covering the entire region. A network of regularly spaced straight lines, each parallel to one of the coordinate axes, is superimposed over the region. Instead of seeking the value of the solution of the differential equation at every point in the continuous region, an attempt is made to determine approximate values of the solution at the mesh points, the intersections of the network lines with each other, and with the boundary of the region.

The partial derivatives of the function of interest, T, at a mesh point are replaced by partial difference quotients; thus, obtaining a linear algebraic equation, called the difference equation, involving the value of T at adjacent points.

As the size of the mesh is made finer, the evaluation of the partial derivatives using the difference quotients can be precise enough so that it would be possible to obtain a difference equation which "approximates well" the partial differential equation.

However, problems of stability and convergence frequently arise in finite difference methods and care must be exercised about both of these problems when selecting the finite difference scheme.

According to the formulas selected for approximating the partial derivatives, the temperatures can be computed either directly from the temperatures of the preceeding nodes or as a solution of simultaneous equations(9). The first of these schemes is called explicit,

while the second is called implicit. Although implicit methods may require the storage of large arrays, they are unconditionally stable and are more reliable than explicit methods for accurate results. Furthermore, they are better suited in problems where large temperature gradients occur since a large temperature gradient is a source of instability in the computation.

In this investigation, where high gradients are expected near the surface of the water chilled ingot, only implicit methods are considered. The main problem is therefore how to solve the set of simultaneous equations $\overline{\overline{M}}\,\overline{T} = \overline{Q}$, $\overline{\overline{M}}$ being the matrix of the coefficients, $\overline{Q}$ being the vector representing the second member of the set of equations, and $\overline{T}$ being the vector whose k^{th} coordinate is the value of the temperatures at the k^{th} mesh point in the region. Such sets of equations can be solved directly by elimination, but this procedure is very inefficient for large sets such as those encountered in this problem. It has been found(10) that iterative procedures are much more efficient than Gaussian elimination when the order of the matrices involved is large. The procedure selected in this investigation is referred to as S.I.P. (Strongly Implicit Procedure) and was first developed for two dimensional heat transfer analysis by H. L. Stone(10).

This method has been chosen for two main reasons. First, it is an unconditionally stable procedure which has been proved to converge even more rapidly than the A.D.I. (Alternating Direction Iteration) method(11) in many cases. Second, a generalization of the S.I.P procedure to three dimensional problems has been recently published(12), making S.I.P. a procedure easily usable for two or three dimensional heat transfer and easily programmable in a computer language. The S.I.P. algorithm in three dimensions is derived in Appendix I.

FORMULATION OF THE PROBLEM

For square (or rectangular) ingot and referring to a coordinate system fixed on the ingot, the general heat equation in transient state can be written(13)

$$\frac{\partial}{\partial x}\left(K\ \frac{\partial T}{\partial x}\right)+\frac{\partial}{\partial y}\left(K\frac{\partial T}{\partial y}\right)+\frac{\partial}{\partial z}\left(K\frac{\partial T}{\partial z}\right)=\rho C_p\frac{\partial T}{\partial t}+Q \qquad (1)$$

where the terms are defined in the nomenclature. This equation governs the heat transfer process and therefore the temperature distribution inside the ingot. Boundary conditions, corresponding to the heat transfer process at the surface of the ingot, must also be specified. This surface heat transfer process can be quite general, and the model does not require any simplification such as constant temperature or constant heat transfer coefficients.

In this investigation, symmetric heat transfer is assumed so that only a quarter of the ingot is considered. When the boundary distribution is chosen, the problem is said to be well posed, and the solution, assumed to exist and to be unique, can be sought.

In the next paragraphs, the assumptions made in the finite difference form of Equation 1 and the treatment of the boundary conditions are examined.

THE TRANSIENT HEAT TRANSFER EQUATION: NUMERICAL APPROACH

The finite difference scheme which corresponds to the S.I.P. algorithm is derived in Appendix II. Its principle is to relate by an implicit equation the temperature at the node (i, j, k) and the six surrounding nodes (see Figure 4) at the new time step to the temperature at the (i, j, k) node at the old time step. The simulation then proceeds in increments of time.

Variation of Physical Properties with Temperature

An important characteristic of this problem is that it involves a phase change. Such problems, where the change occurs at a single temperature or over a temperature range, are sometimes referred to as Stefan's problems and have been of interest to engineers and scientists for a long time(7,8,14,15).

In the case of a pure material, where the phase change occurs at a specific temperature, the properties of the material show a discontinuity at this temperature. The correct mathematical formulation is therefore solving two partial differential equations and an

Figure 4

Typical grid element.

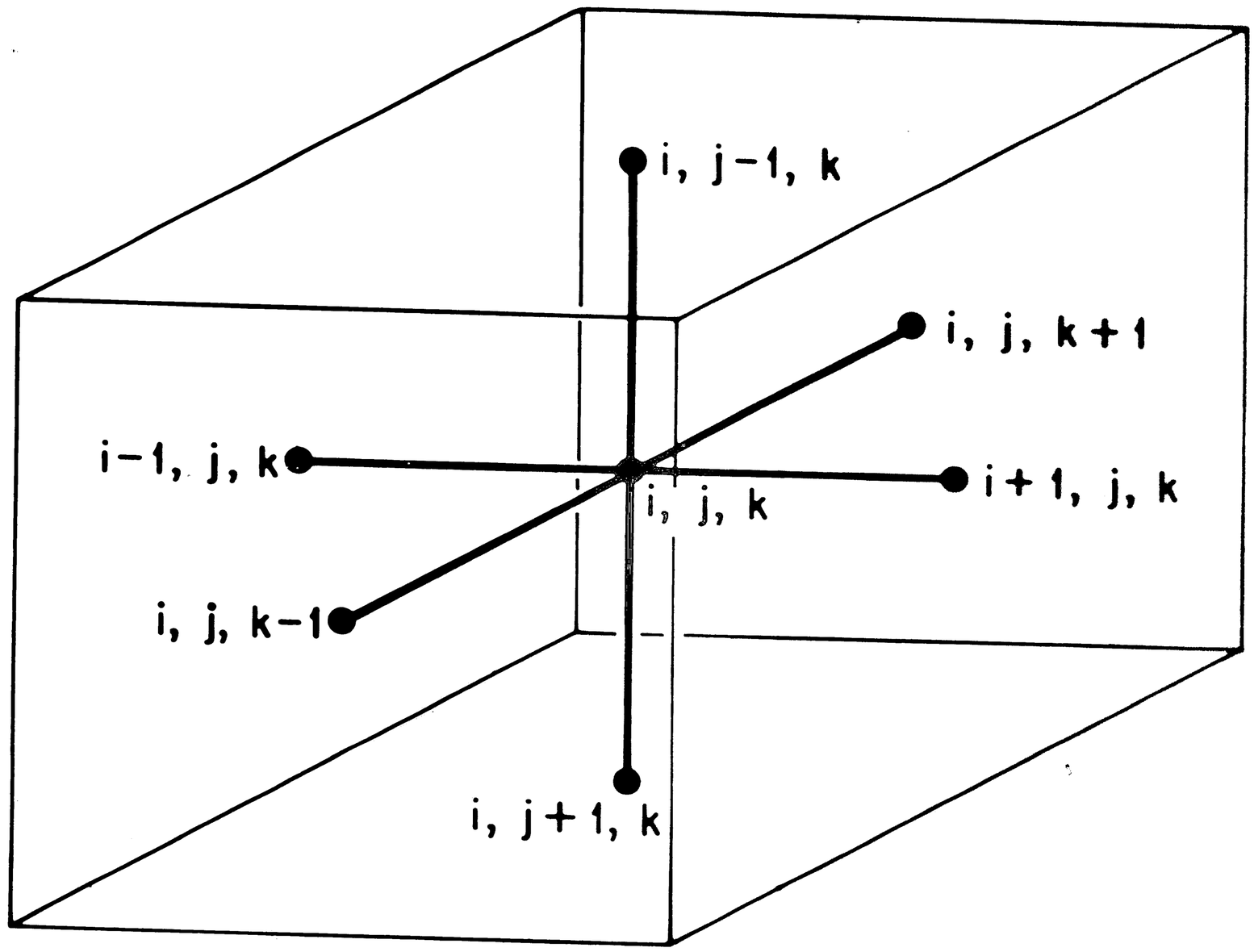
i, j-1, k
i, j, k+1
i-1, j, k
i+1, j, k
i, j, k
i, j, k-1
i, j+1, k

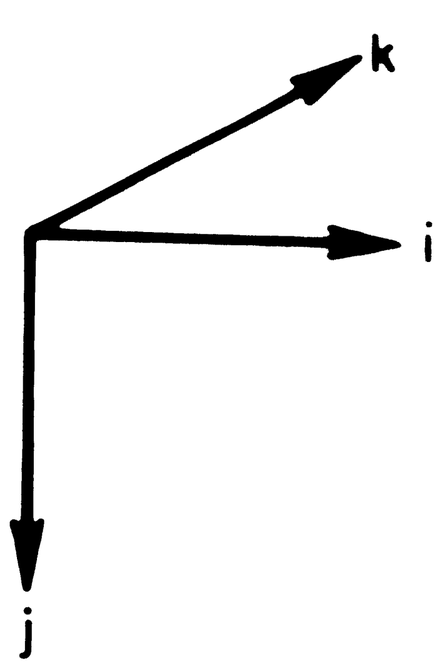
k
i
j

interface equation(14). This would result in serious limitations in our ability to solve such problems. Fortunately, in the case of alloys, the phase change occurs over a temperature range and the properties can be made continuous in the whole temperature range of interest.

The present model can, therefore, handle any variation of the properties with temperature provided these properties are continuous in the two-phase region. In the investigation, where the simulation of the solidification of 308L stainless steel is reported, the variation of thermal conductivity, specific heat, and density of this alloy are shown in Appendix III. Since the values of physical properties of solid or liquid steel at elevated temperature are difficult to obtain, the best data available in the literature for the grade of steel of interest or a similar grade were selected and a simple linear relationship was considered for variation of properties in the "mushy" zone.

A simplification has been introduced to take into account the magnetic or mechanical stirring which might occur in the molten metal pool. Instead of adding a convective term in the equation, the concept of "effective thermal conductivity" was used. The effective thermal conductivity Ke is given by $Ke = K_{conduction} \times K_{convection}$.

Although some investigators claim that the stirring process in the metal pool is almost nonexistent, it is believed that it has a greater importance in the particular process which is studied here since the water cooled mold has been isolated and the lines of current are running through the molten metal.

The heat of fusion L_H is assumed to be released in a linear manner between the solidus and the liquidus temperature. By this we mean that the heat capacity of the mushy zone is adjusted to the value:

$$C_P + L_H / (T_{liq} - T_{sol}).$$

This essentially corresponds to a linear variation of the enthalpy of the steel in the two-phase region. This assumption does introduce a discontinuity in the value of the heat capacity as a function of temperature. However, no important disturbances have been noticed in the results due to this discontinuity. A finer mesh size takes care of the possible oscillation in the temperature of the nodes located in the "mushy" zone.

Boundary Conditions

However complex the process might be, the influence of the experimental parameters is limited to a change in one or several of the six boundary conditions corresponding to the mechanisms of heat transfer at the six planar surfaces of the ingot.

Centerplanes of the Ingot

Since a symmetric heat transfer is assumed, only a quarter of the ingot is considered. As shown in Figure 5, the boundary condition is therefore $\frac{\partial T}{\partial x} = 0$ on the plane $x = X$; similarly, the boundary condition is $\frac{\partial T}{\partial z} = 0$ on the plane $z = Z$.

Slag Metal Interface

The heat transfer at the slag metal interface is a very complex one. Some insight has been given on this subject by Dudko and coworkers(16) and more recently by Campbell(17). The main conclusion seems to be that most of the heat transfer to the metal pool takes place via the molten metal droplets and not via a normal heat transfer process at the slag metal interface. Some experimental data by Sun(5) showing a rather sharp discontinuity between the temperature in the slag and in the metal pool at the interface would lend support to the above suggestion. In view of this still unsolved problem of the actual heat transfer process at the slag metal interface, a constant temperature was selected as a boundary condition. This corresponds to droplets having a constant superheat. The fact that the temperature is taken as uniform at the top of the metal pool could be justified by the back and forth movement of the electrode in the mold which

Figure 5

Boundary conditions.

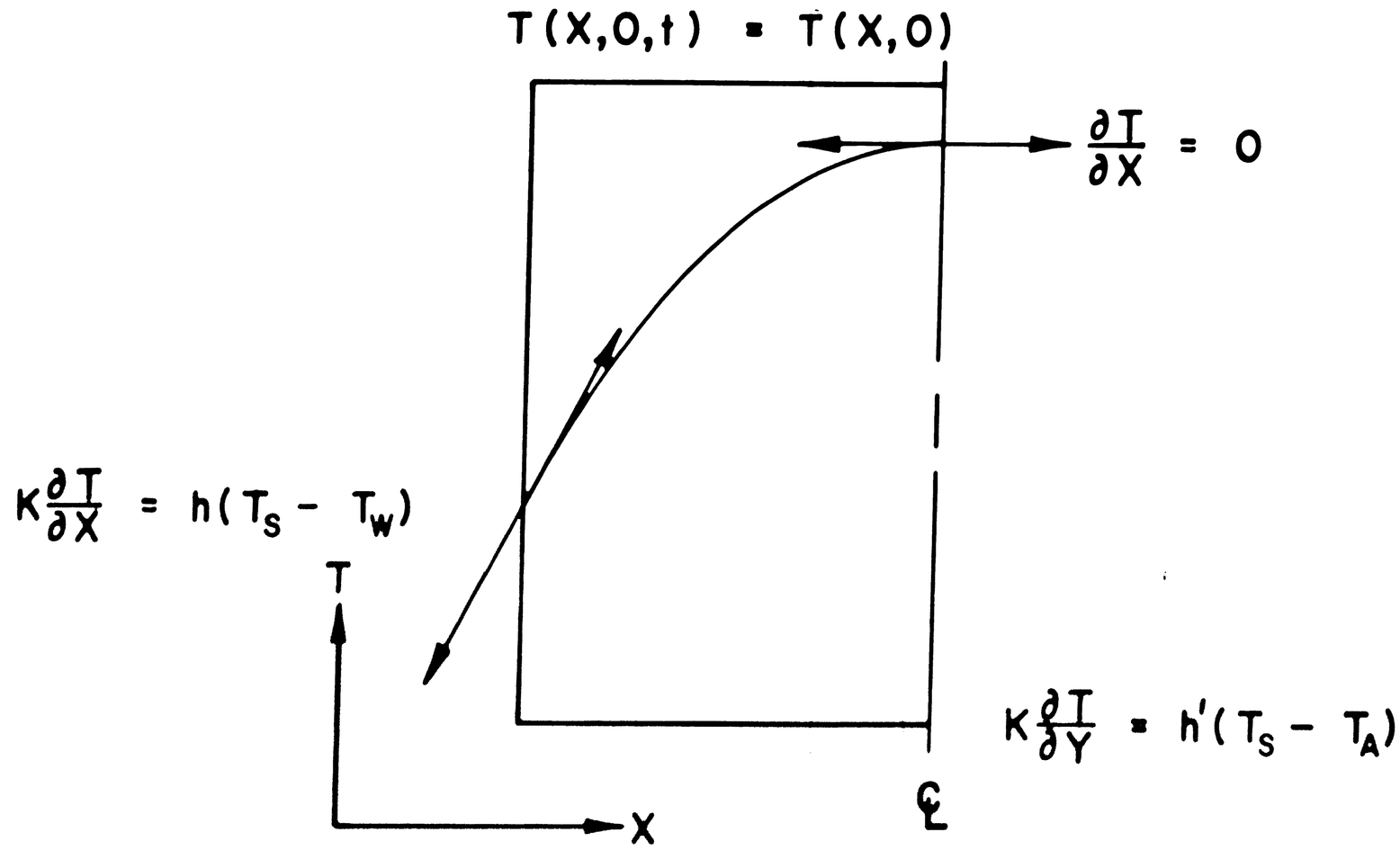
T(X,0,t) = T(X,0)
$\frac{\partial T}{\partial X} = 0$
$K\frac{\partial T}{\partial X} = h(T_S - T_W)$
T
X
℄
$K\frac{\partial T}{\partial Y} = h'(T_S - T_A)$

evenly distributes the droplets through the whole section of the ingot; it is however considered to be an approximation, which will be refined when considering the three-dimensional model.

Heat Transfer in the Mold

The heat transfer process, otherwise rather simple, in the mold is affected by two things. First the existence of a thin slag skin due to the solidification of the slag at the surface of the mold near the slag metal interface. Second the possible existence of a gap after the ingot contracts away from the mold. Furthermore, a bad surface finish can drastically reduce the heat transfer coefficient as has been noticed in several experiments.

Some experimental data published by Sun(5) give an upper and lower bound for the heat transfer coefficient between the mold and the ingot through a slag skin. These values, however, do not take into account the air gap. Several heat transfer coefficients have been selected, and their effect on the temperature distribution simulated on the computer.

Heat Transfer in the Sprayed Zone

As soon as the ingot enters the sprayed zone, its temperature drops very rapidly. Most of the heat released is used to vaporize the sprayed water. This vaporization continues until the temperature of the ingot drops below 212°F. Then the water is simply running on the surface of the ingot, and the amount of heat extracted is much lower. The model has to take these two different types of heat transfer into account, and two values of the heat transfer coefficient were selected, according to the temperature of the ingot. Because of the lack of data available and of the difficulty of measuring the amount of water vaporized, an empirical value was selected which gives reasonable temperature values. The only possible correlation between the results of the simulation and the experiments is the fact that the temperature of the ingot surface is in the range 100-150°F below the sprayed zone.

Treatment of the Downward Movement of the Ingot

The extraction of the solidified ingot through the mold and the continuous flow of liquid metal droplets into the pool can be simulated by making the following translation in the temperature distribution at every time step:

$$T(i, j, k) = T(i, j-n\Delta y, k) \quad (1)$$

for all i, j, k with $n\Delta y = V\Delta t$ (2)

and depositing a thin layer of hot metal at the top of the pool (for values of j between 1 and $n\Delta y$). This corresponds to a discretization of the downward movement of the ingot, which is necessary since the time coordinate has been discretized for the need of finite difference method. This method, however, has a very serious drawback due primarily to Equation 2. n being an integer > 1, the highest value of Δy is $V\Delta t$. The size of Δt is limited by accuracy requirements, and the speed of extraction V is very low. Hence, the resultant upper bound for the mesh size in the y direction is also very low. Furthermore, due to Equations 1 and 2 a constant mesh size is required in the y direction.

Several runs of a two dimensional analysis of the problem show an optimum time increment of 10 to 15 seconds. With a speed of extraction of 0.5 inch per minute, the maximum mesh size in the y direction would be 0.083 inch. This mesh size is much too small to allow the simulation to be undertaken with reasonable computer time and memory requirements. Instead, the downward movement of the ingot represented by Equation 1 and 2 was performed every three time steps so that a reasonable mesh size could be used. This method is not, however, completely satisfactory because of the lack of accuracy in the determination of the depth reached by the pool shape after the simulation has proceeded for a certain length of time. In other words, the steady state is difficult to detect in the computer output.

Another shortcoming of this method is the need for a good guess for the initial temperature distribution to avoid prohibitive time requirements. Despite these two shortcomings, the method can

give a good approximation of the heat transfer process at the beginning of a melt, when the ingot is of short length. Furthermore, if the steady state could be predicted by some other way, it would give an idea of the dynamic behaviour of the process.

A STEADY STATE HEAT TRANSFER MODEL OF THE PROCESS

The need for a steady state analysis was expressed in the above paragraph. The first question which must be asked concerns the existence of a steady state. The answer is obvious for physical reasons; if the parameters of the process are kept constant and after the ingot has reached a minimum length so that the end effects on the shape of the pool are negligible, a steady pool shape is attained. Such a pool shape is the result of a temperature distribution which is the solution of the following heat transfer equation (see Appendix II, B for derivation):

$$\frac{\partial}{\partial x}\left(K\frac{\partial T}{\partial y}\right)+\frac{\partial}{\partial y}\left(K\frac{\partial T}{\partial y}\right)+\frac{\partial}{\partial z}\left(K\frac{\partial T}{\partial z}\right)=\rho C_p V\frac{\partial T}{\partial y}+Q \qquad (3)$$

where T is a function of the three space variables only.

Unlike the time dependent equation, the solution of this equation is not dependent on the initial temperature distribution and gives the steady state distribution corresponding to the boundary conditions selected. The finite difference form of Equation 3 is very similar to the difference form of Equation 1 and the resulting algorithm and computer program are very similar. As usual in this kind of problem, the iteration scheme corresponding to the elliptic equation (Equation 3) converges much more slowly than for the corresponding parabolic equation (Equation 1). Nevertheless, the interpretation of the results of the steady state analysis is much more reliable than in the dynamic case. The influence of process parameters can be shown and interpreted more readily as will be discussed in Section III.

COMPUTER PROGRAMMING

A computer program was written for a two and three dimensional heat transfer approach of the model. The two dimensional analysis essentially corresponds to the solution of the heat transfer equation in an infinitely long slab, whose width is equal to the width of the ingot considered. Typical computer memory requirements for the simulation of a 4 inch x 12 inch slab is on the order of 60,000 octal words. Typical computer times for the steady state analysis are 30 to 40 seconds for each run, with a reasonably good initial guess. The convergence of the algorithm in the steady state case is much slower than for the dynamic case. (20 to 30 iterations were needed in order to obtain a fairly good accuracy of the solution.) Since the process which was intended for simulation usually casts 4 inch x 4 inch ingots and since several experiments have been made with a 4 inch square ingot, a three dimensional analysis was run to check the correlation between experimental and theoretical results. Although the mesh size has been slightly increased in comparison to the two dimensional model, the memory requirement is on the order of 120,000 octal words which almost saturates the CDC 6400, Lehigh University's computer. Furthermore, each iteration takes approximately 10 seconds of computer time; so that a single run of the three dimensional model is rather costly.

Only a few runs were performed with several melting rates, since the melting rate seems to be the parameter to which the model is most sensitive. The listings of the computer programs have not been included in this presentation. However, information about the programming techniques can be obtained by contacting the author or the Department of Metallurgy and Materials Science of Lehigh University where copies of the computer program have been left on file with Professor W. C. Hahn.

EXPERIMENTS

The continuous electroslag remelting process has not been studied very extensively. Therefore, the relation between the pool depth and the process parameters, particularly the speed of extraction, was not quantitatively known. An experiment consisting in doping the molten pools with sulfur for two different speeds of extraction and two different slag pool depths was carried out during the remelting of a 4 inch x 4 inch square 308L ingot. The ingots were then sawed in half so that sulfur prints could be taken of the molten metal pools. The four samples corresponding to each speed of extraction and each slag pool depth were also macroetched in order to reveal the solidification pattern. The two melt rates selected were 2.2 Lb/mn and 1.7 Lb/mn corresponding respectively to an extraction rate of 31 inches per hour and 24 inches per hour. The two slag depths were measured as 2.5 inches and 4.0 inches.

The sulfur prints (as shown on Figure 6.a) gave the results shown in Table I. They show, as was expected, that the pool depth is highly influenced by the melt rate. They do not show, however, any dependence of the pool depth on the amount of slag as is reported for the conventional ESR process. A sulfur print of the ingot on a horizontal cross section shows (Figure 6.b) how the shape of the pool is influenced by the corners of the ingot. Once the shape of the horizontal and vertical cross section of the metal pool is obtained, the results of the two and three dimensional programs can be interpreted and compared to the experimental results.

Figure 6

Some experimental pool shapes obtained by sulfur print:

a Vertical sections

b Transverse section

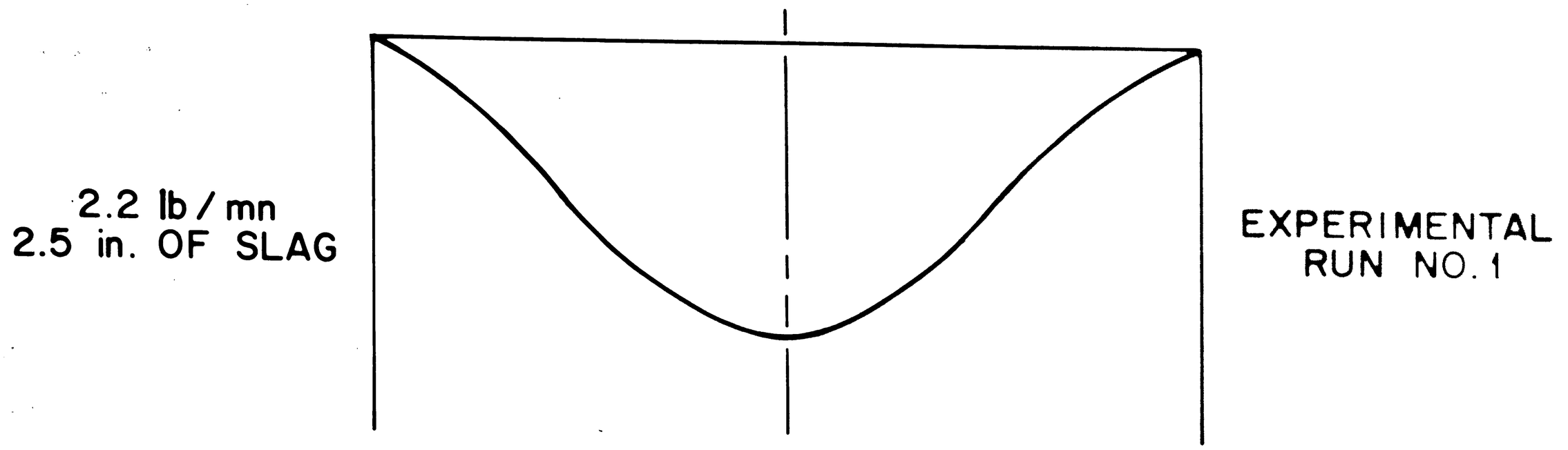
2.2 lb / mn
2.5 in. OF SLAG
EXPERIMENTAL
RUN NO. 1
2.2 lb / mn
4.5 in. OF SLAG
EXPERIMENTAL
RUN NO. 2
SECTION SHOWN
ON FIG. 6-b
1.7 lb / mn
4.5 in. OF SLAG
EXPERIMENTAL
RUN NO. 3

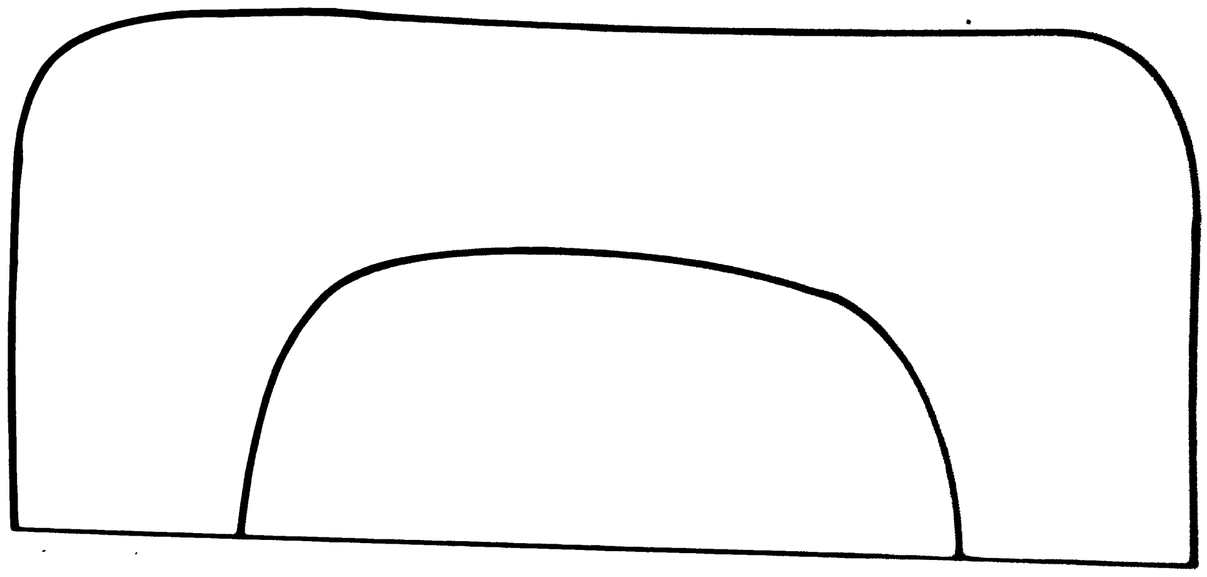

EXPERIMENTAL RUN NO.2

TRANSVERSE SECTION OF THE INGOT 0.9 in. BELOW POOL SURFACE.

TABLE I

RESULTS OF POOL DEPTH MEASUREMENTS BY SULFUR PRINT

Slag Depth \ Melting Rate	1.7 Lb/mn	2.2 Lb/mn
2.5 inches	0.9 inch	1.4 inches
4.0 inches	0.9 inch	1.4 inches

MODEL RESULTS

Five parameters were varied independently and their impact on the temperature distribution was studied. These five parameters were:

the speed of extraction (or melt rate)
the temperature of the slag-metal interface
the heat transfer coefficient of the mold
the length of the mold
the heat transfer coefficient of the spray.

The change in the steady state temperature distribution was calculated using a two dimensional analysis of the problem. The two dimensional approach was selected because the memory and time requirements are reasonable as was discussed earlier. Furthermore, the resulting computer program is simpler and can be used much more easily to find reasonable values for some coefficients in the model. These coefficients are the heat transfer coefficient at the mold metal interface and in the sprayed zone, and the temperature of the slag metal interface. The two dimensional model has been also used to select a mesh size which would give a good accuracy and yet be conservative of computer memory. The mesh size has been also selected to avoid oscillation of the temperature at the nodes located at the liquid-solid metal interface. This oscillation is due to the release of the heat of fusion between the solidus and the liquidus temperatures. It can be avoided only by selecting a finer mesh size and by letting the iteration procedure run a few more times. Finally, a stable temperature distribution corresponding to the steady state is obtained.

The results of the two dimensional program are treated in the next paragraph.

TWO DIMENSIONAL PROGRAM - RESULTS

Before investigating the effect of different parameters on the temperature distribution of the ingot, several preliminary runs were

made to select reasonable values of the important process parameters (heat transfer coefficient in the mold, heat transfer coefficient of the spray, temperature at the slag metal interface).

A superheat varying from 50°F to 200°F was found to be a reasonable value for the temperature of the droplets at the slag metal interface. The possibility of a rather high degree of superheat is due to two reasons. First some of the material being remelted arrives in the slag in the form of powder, and therefore presents a high surface to volume ratio. These fine particles are going to fall down through the slag at a rather low speed, and their temperature will increase appreciably since the temperature of the slag, as measured by an optical pyrometer averages 3200°F to 3300°F. Second the strip which is continuously fed into the pool and forms most of the remelted product is a low carbon steel, whose liquidus temperature is approximately 100°F higher than the liquidus temperature of 308L. A surface temperature of 2700°F to 2800°F (100°F to 200°F of superheat) was therefore considered to be a valid assumption on the temperature of the slag metal interface.

A common value for heat transfer coefficients between the slab and the copper mold in a continuous casting mold is 200 $Btu/ft^2/Hr/°F$. This value however gives results which are out of range for the continuous electroslag remelting process. A value of 30 to 60 $Btu/ft^2/Hr/°F$ seems to be much more realistic. This value is in agreement with the results of Sun(5) who measured experimentally and then simulated the heating curves of slag coated copper rods immersed in a liquid metal.

The heat transfer coefficient in the sprayed zone is very much dependent on the intensity of the spray. It is believed to vary from 50 $Btu/ft^2/Hr/°F$ for a very light and diffuse spray to 400 $Btu/ft^2/Hr/°F$ for a high strength spray. A typical set of isotherms obtained with the values selected is shown on Figure 7.

Figure 7

Typical set of isotherms as obtained by the computer model.

Process parameters:

extraction speed: 10 in/h

heat transfer coefficient in the mold = 50 Btu/ft^2/Hr/°F

heat transfer coefficient in the sprayed zone: 400 Btu/ft^2/Hr/°F

temperature at the slag metal interface: 2700°F

grade of steel: 308L stainless steel

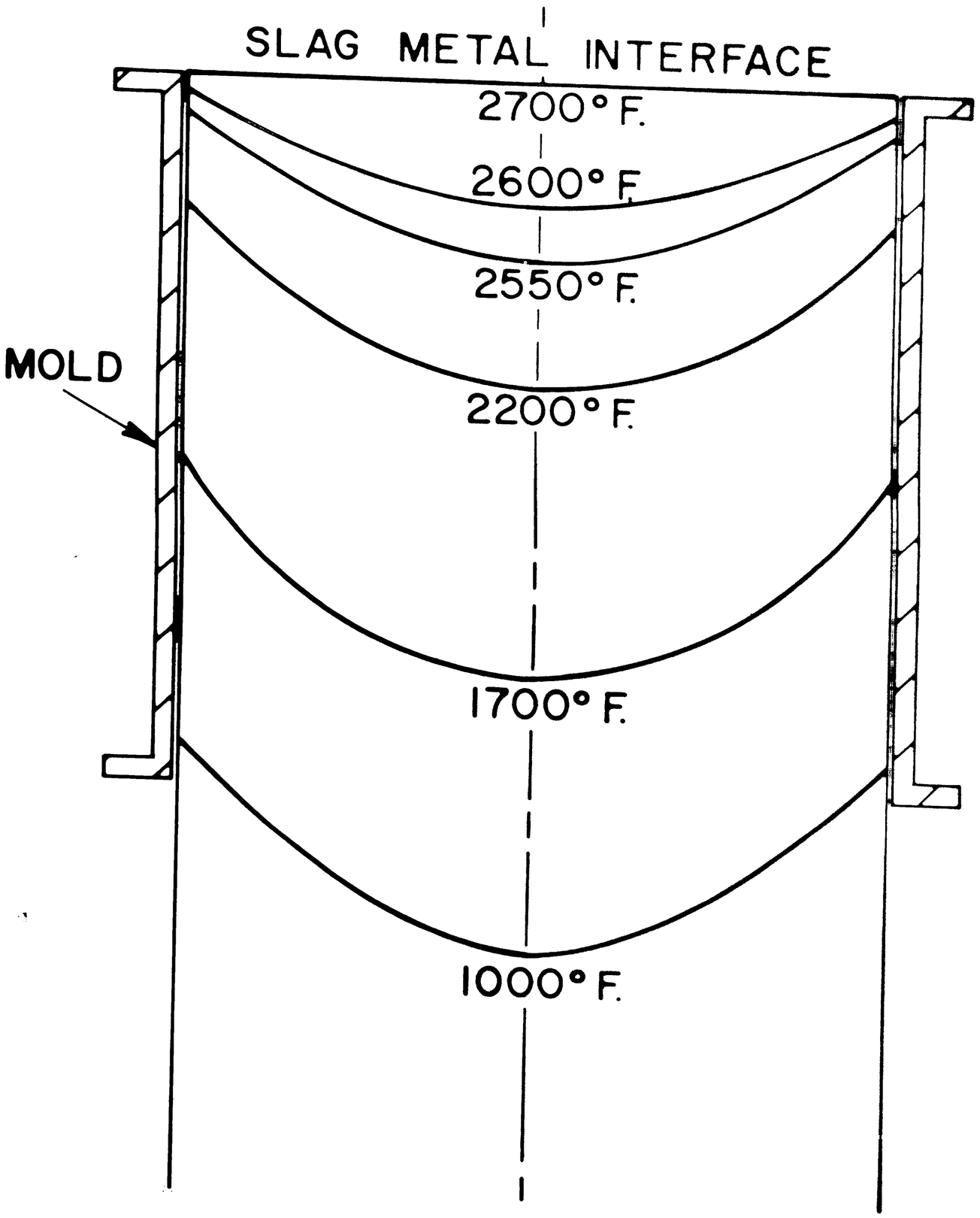
SLAG METAL INTERFACE
2700° F.
2600° F.
2550° F.
MOLD
2200° F.
1700° F.
1000° F.

Influence of the Melting Rate on the Temperature Distribution

The melting rate has a profound influence on the temperature distribution and especially on the shape of the molten metal pool. The computer program was run for three melting rates corresponding to extraction speeds of 10, 24 and 30 inches per hour. These speeds correspond to the rate of extraction of the ingot generally encountered in electroslag remelting. Figure 8 shows the different pool shapes obtained at these three different speeds. In these three computer runs, the only variable was the speed of extraction, and Figure 9 shows a linear relationship between the depth of the pool and the speed of extraction. This linear relationship agrees with the prediction of Biochenko(18) quoted by Chalmers(19) that the depth of the liquid pool is proportional to the rate of casting. We will discuss later the limitations of this theoretical linear relationship for an actual operating process. In Figure 10, the temperature at the centerline of the ingot and along the surface of the ingot has been plotted for the three different extraction speeds. Since we are interested in the steady state conditions, distance along the centerline of the ingot and time are equivalent quantities so that the slope of the curves in Figure 10 also represents the cooling rate of a point along the surface and along the centerline of the ingot. For an extraction speed of 24 inches per hour, the cooling rate is found to be 100°F per minute at the center of the ingot. At the surface, it varies from 70°F per minute in the mold to 500°F per minute in the sprayed zone.

It is interesting to note that an extraction speed of 10 inches per hour provides a homogeneous cooling through the whole ingot. The cooling rate is equal to 40°F per minute. This proves that a low extraction speed can provide a very homogeneous solidification pattern.

Temperature at the Slag Metal Interface

Several amounts of superheat were selected and their influence on the temperature distribution in the ingot was studied. If the surface conductance value between the ingot and the mold is

Figure 8

Pool shape for different speeds of extraction.

Process parameters:

extraction speed = 10,24,40 in/h

heat transfer coefficient in the mold = 50 Btu/ft^2/Hr/°F

heat transfer coefficient in the sprayed zone = 400 Btu/ft^2/Hr/°F

temperature at the slag metal interface: 2700°F

grade of steel: 308L stainless steel

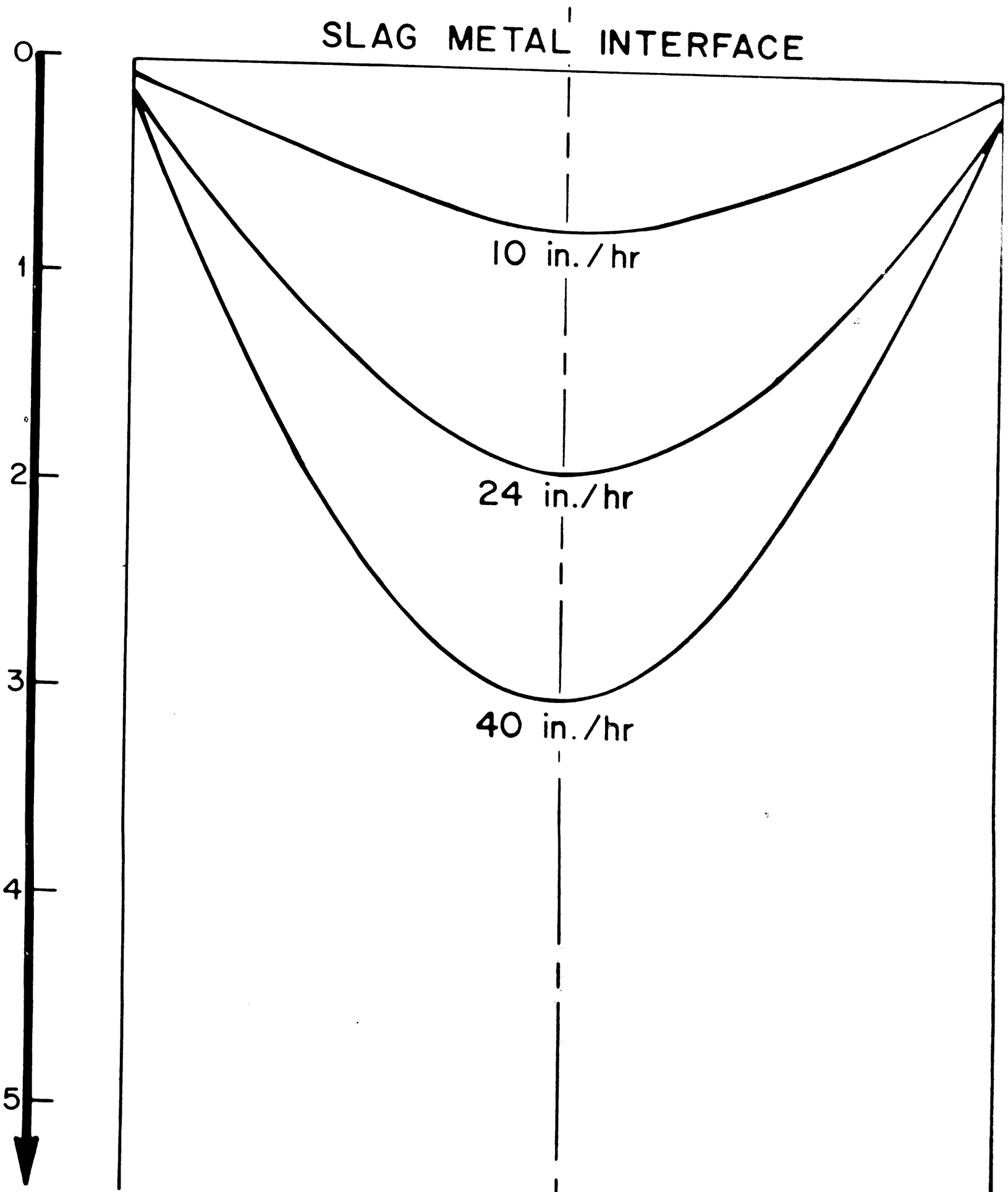
SLAG METAL INTERFACE
0
1
2
3
4
5
INCHES
10 in./hr
24 in./hr
40 in./hr

Figure 9

Dependence of the metal pool depth on the speed of extraction of the ingot.

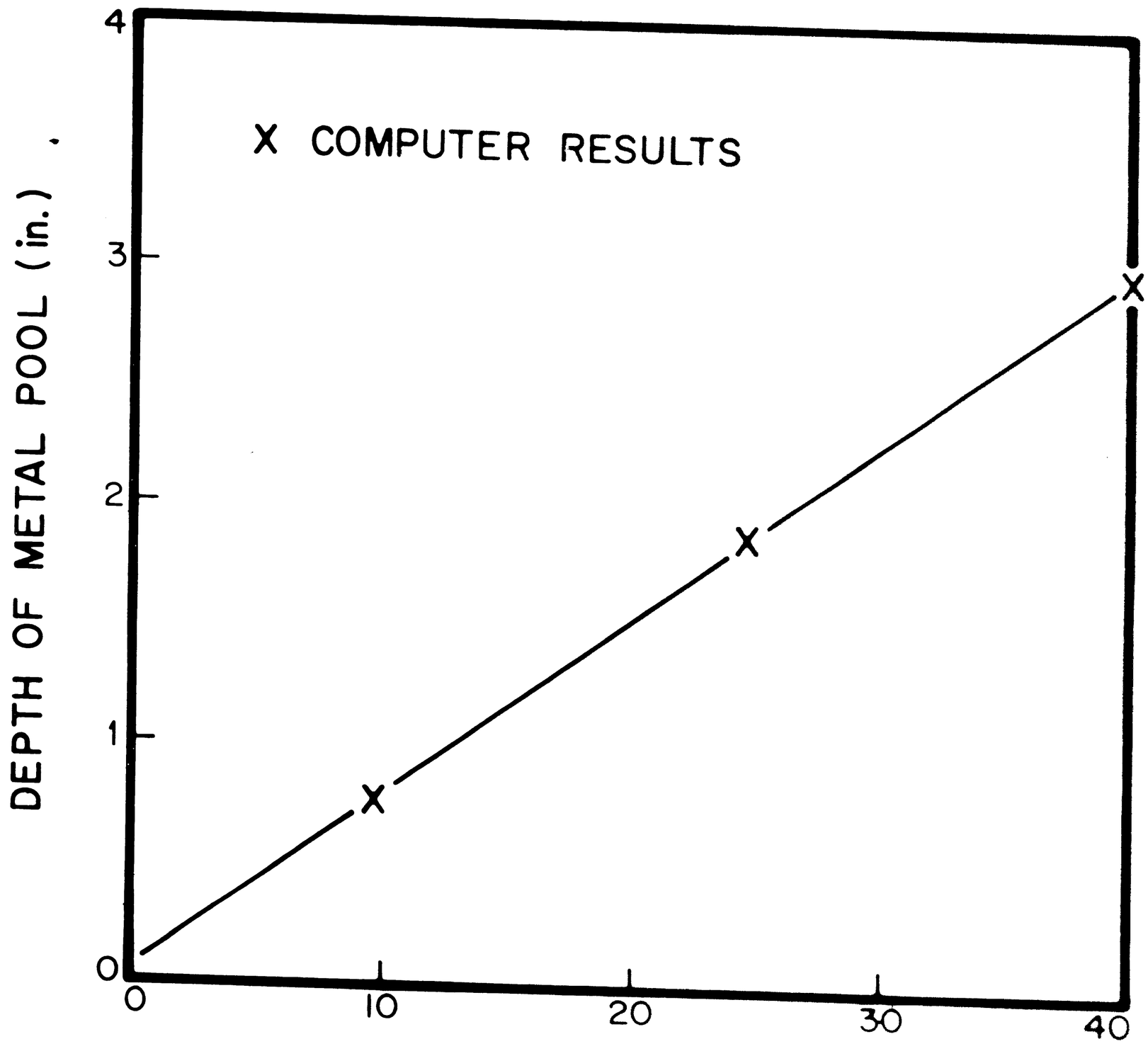
X COMPUTER RESULTS
DEPTH OF METAL POOL (in.)
0
1
2
3
4
0
10
20
30
40
SPEED OF EXTRACTION (in./hr)

Figure 10

Temperature profiles along the centerline and on the surface of the ingot for different extraction speeds.

Curves No. 1 Indicate the temperature profile on the surface.

Curves No. 2 Indicate the temperature profile along the centerline.

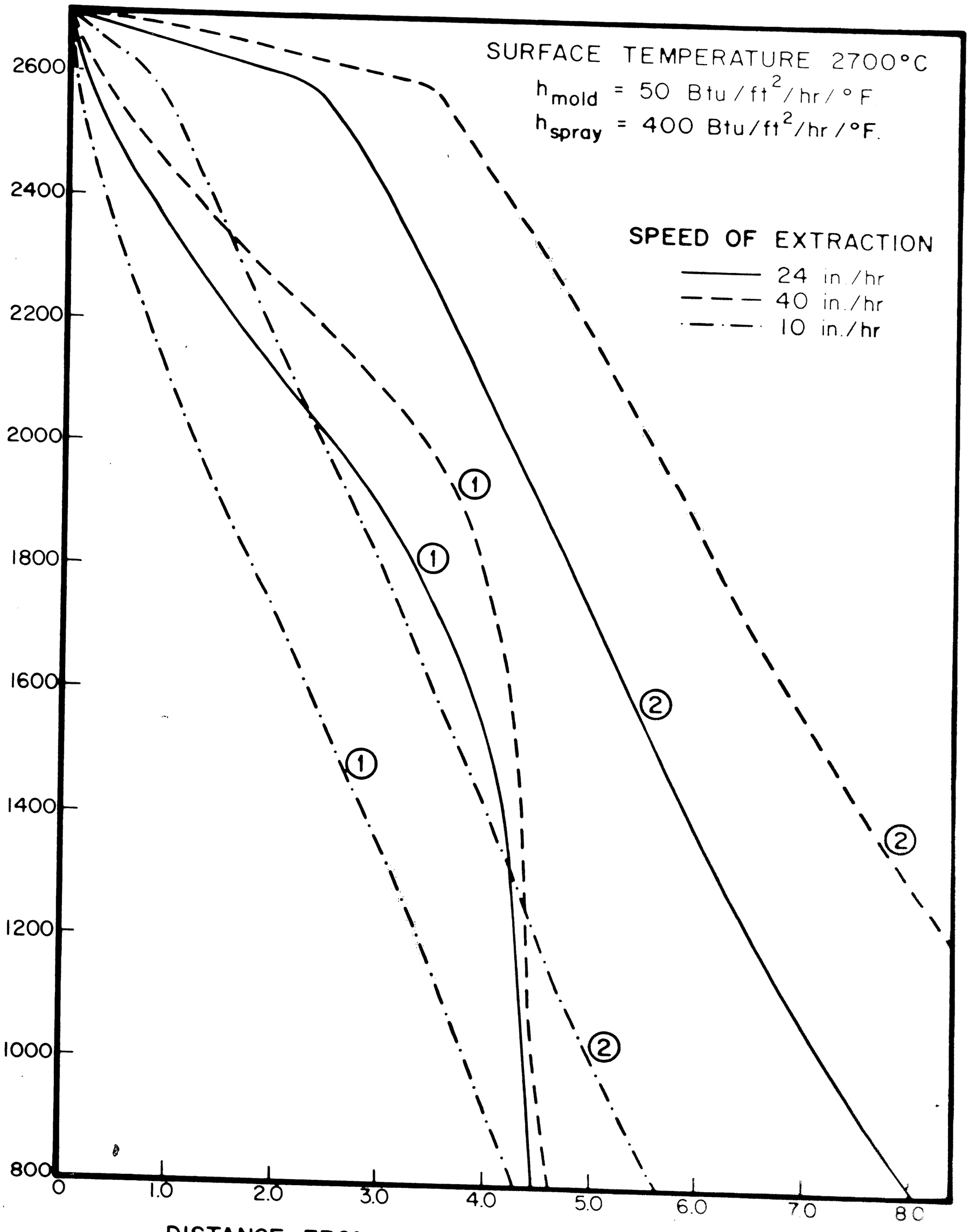
SURFACE TEMPERATURE 2700°C
h_{mold} = 50 Btu/ft²/hr/°F
h_{spray} = 400 Btu/ft²/hr/°F
SPEED OF EXTRACTION
24 in./hr
40 in./hr
10 in./hr
TEMPERATURE (°F.)
2600
2400
2200
2000
1800
1600
1400
1200
1000
800
0
1.0
2.0
3.0
4.0
5.0
6.0
7.0
8.0
DISTANCE FROM THE SURFACE OF THE INGOT (in.)
①
②

considered constant, the amount of superheat does not affect the temperature distribution very much, as shown in Figure 11.

Heat Transfer Coefficient in the Mold

Figure 12 shows the influence of two different heat transfer coefficients on the temperature profiles in the ingot. It can be noted that the temperature distribution is rather sensitive to a change in the mold heat transfer coefficient. A more detailed study of the influence of the surface finish on the shape of the pool will be done in the three dimensional analysis of the problem.

Influence of Length of Mold

Although the length of the water cooled mold in the electroslag process is of much less importance than in continuous casting because of the much slower speed of extraction, it is worth considering how much it influences the temperature distribution. As can be seen in Figure 13, the mold length does not have an important effect on the metal pool depth. It does, however, have an important influence on the rate of solidification of the ingot, and on the surface temperature at the end of the mold. It is therefore an important factor which provides a good means of controlling the rate of solidification of the ingot. Furthermore, the temperature at which the ingot reaches the spray (temperature T_1, T_2, T_3 on Figure 13) can also be controlled by selecting a mold of determined length.

THREE DIMENSIONAL PROGRAM - RESULTS

After the two dimensional analysis of the problem was tested and some more insight given to the influence of the process parameters on the temperature distribution inside the ingot, a three dimensional program taking into account the heat transfer in the three space directions was run on the computer. As was mentioned earlier, this program was merely a generalization of the two dimensional one, and the same assumptions and computational procedures were used. The mesh size, however, had to be increased slightly in order to run the program on

Figure 11

Influence of different amounts of superheat on the temperature profile along the centerline and on the surface of the ingot.

Curves No. 1 Temperature profile on the surface of the ingot.

Curves No. 2 Temperature profile along the centerline of the ingot.

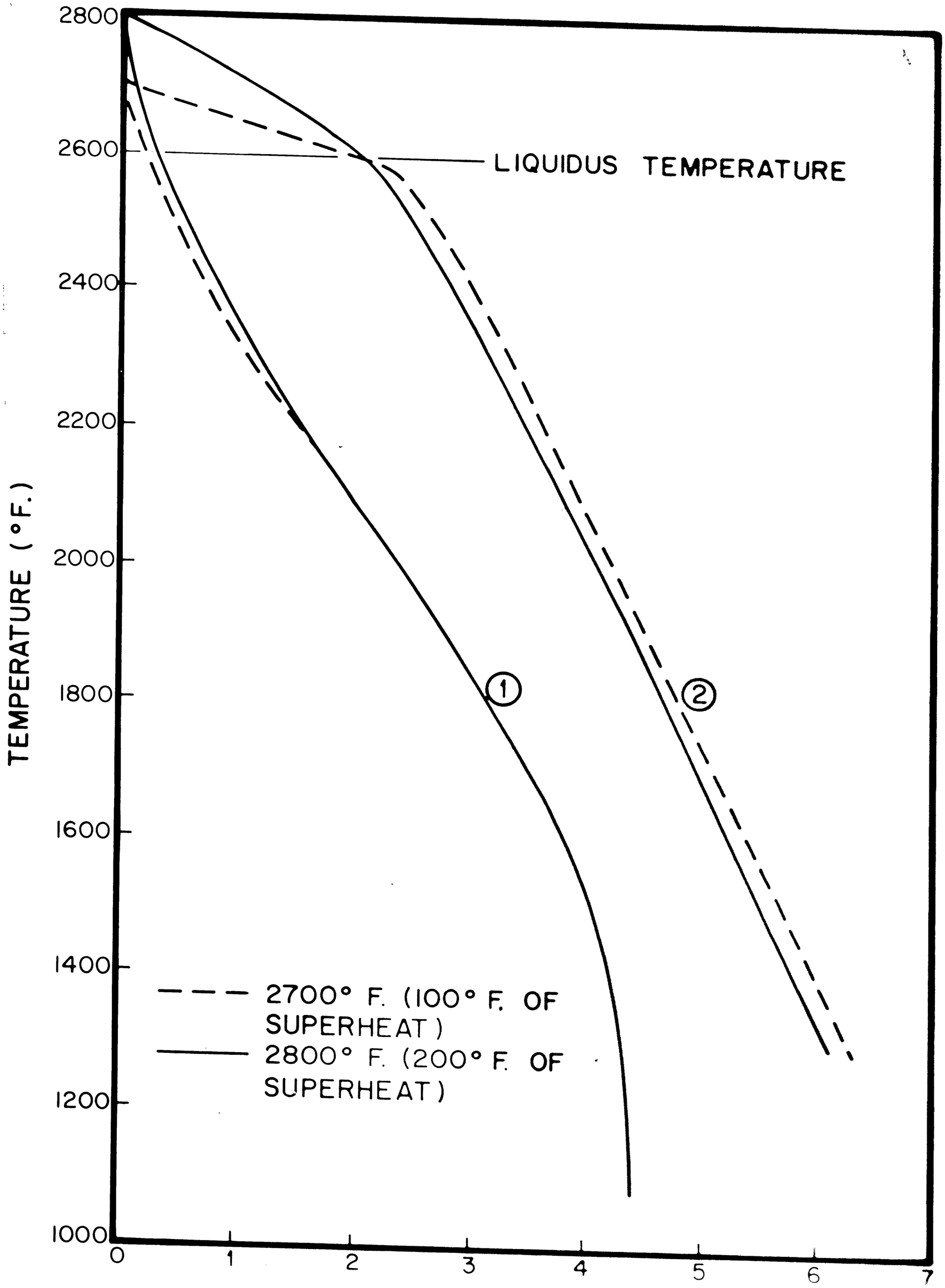
2800
2600
2400
2200
2000
1800
1600
1400
1200
1000
TEMPERATURE (°F.)
LIQUIDUS TEMPERATURE
①
②
2700° F. (100° F. OF SUPERHEAT)
2800° F. (200° F. OF SUPERHEAT)
0
1
2
3
4
5
6
7
DISTANCE FROM THE SLAG METAL INTERFACE (in.)

Figure 12

Influence of different heat transfer coefficients between ingot and mold on the temperature profiles along the centerline and on the surface of the ingot.

Curves No. 1 Temperature profiles on the surface of the ingot.

Curves No. 2 Temperature profiles along the centerline of the ingot.

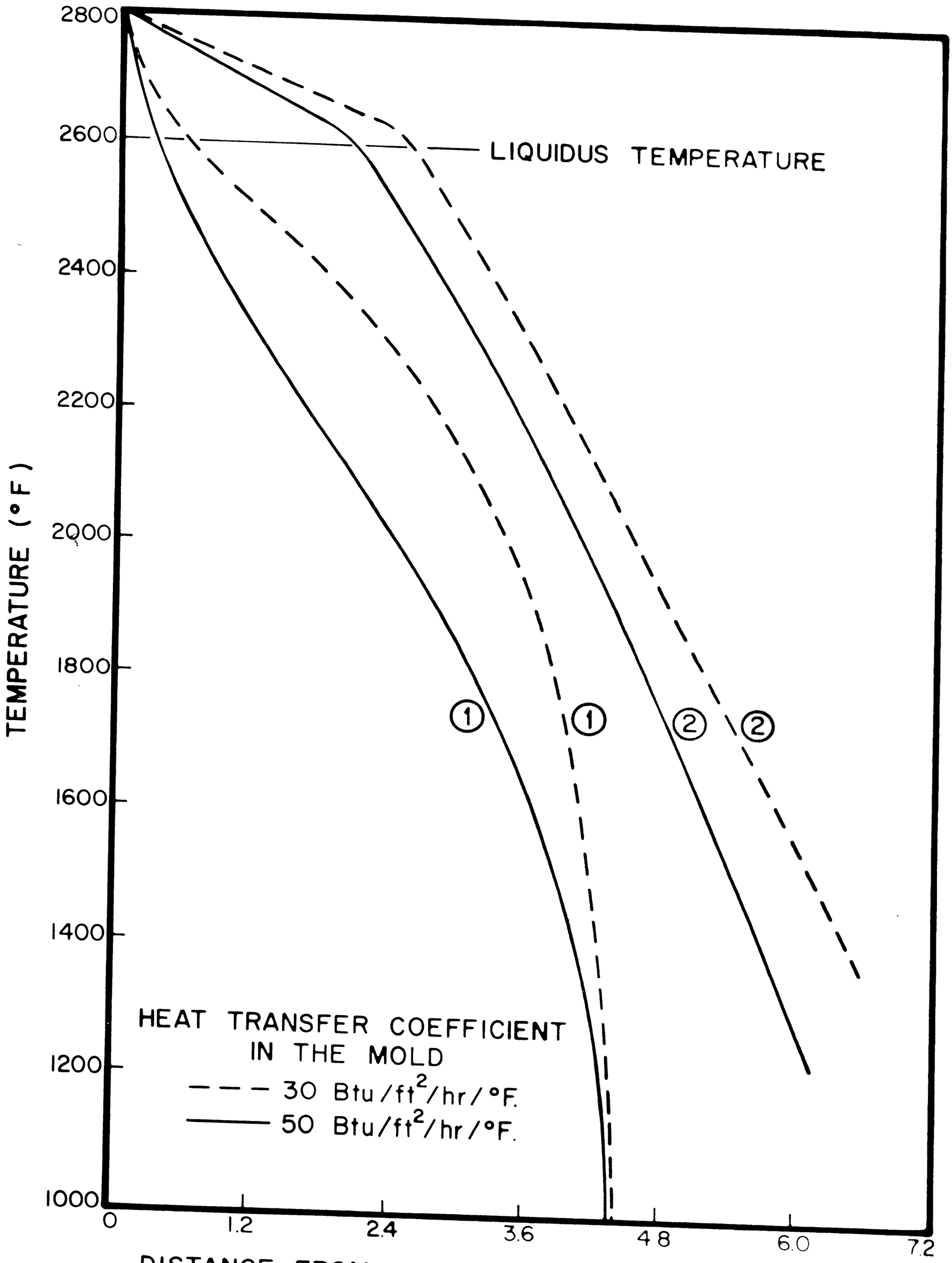
2800
2600
2400
2200
2000
1800
1600
1400
1200
1000
TEMPERATURE (°F)
LIQUIDUS TEMPERATURE
1
1
2
2
HEAT TRANSFER COEFFICIENT
IN THE MOLD
--- 30 Btu/ft²/hr/°F.
——— 50 Btu/ft²/hr/°F.
0
1.2
2.4
3.6
4.8
6.0
7.2
DISTANCE FROM THE SLAG METAL INTERFACE (in.)

Figure 13

Influence of the length of the mold on the temperature profile along the centerline and on the surface of the ingot.

Curves No. 1 Surface temperature.

Curves No. 2 Temperature profile along the centerline.

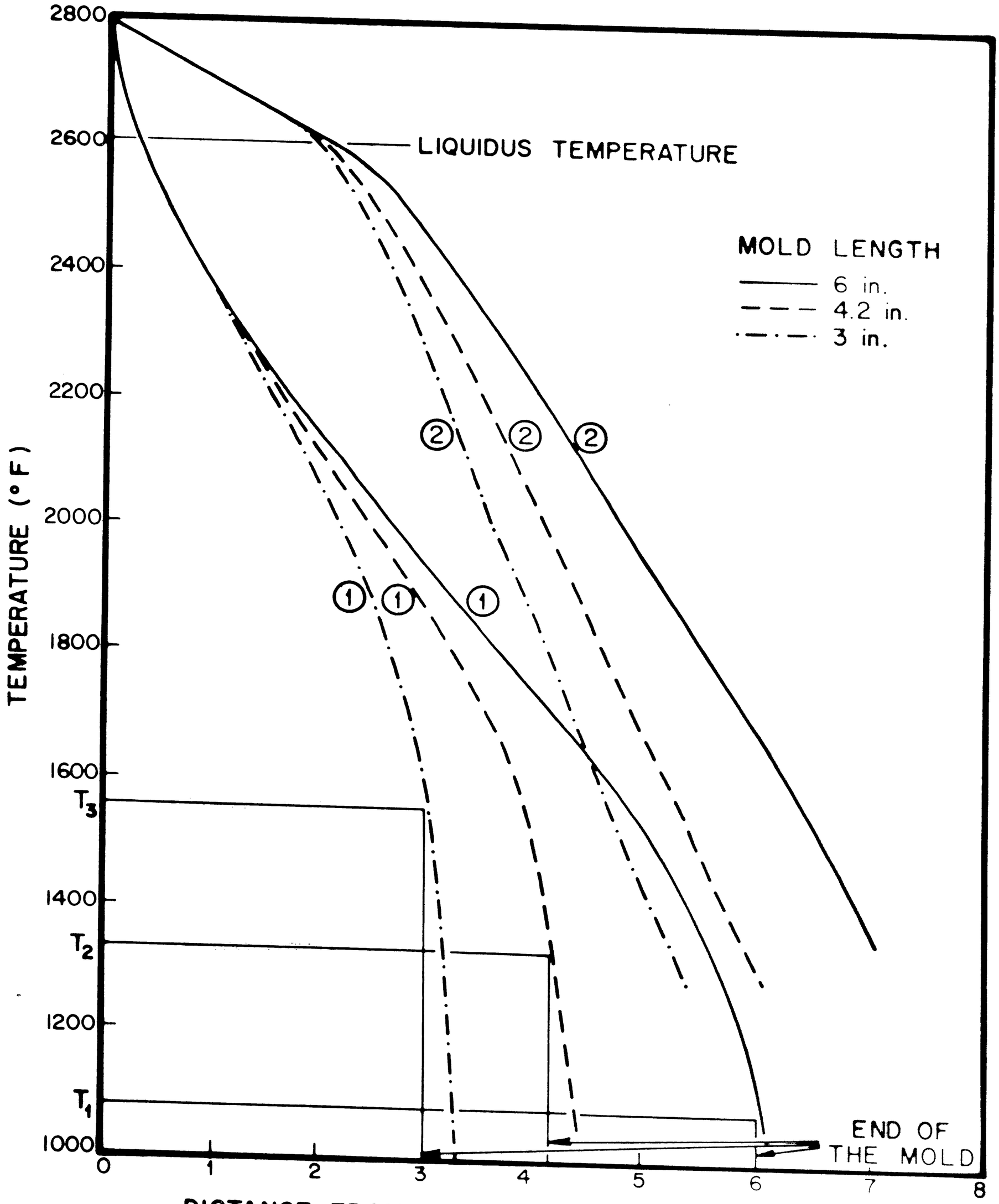
2800
2600
2400
2200
2000
1800
1600
1400
1200
1000
TEMPERATURE (°F)
LIQUIDUS TEMPERATURE
MOLD LENGTH
6 in.
4.2 in.
3 in.
T3
T2
T1
1
2
END OF THE MOLD
0
1
2
3
4
5
6
7
8
DISTANCE FROM THE SLAG METAL INTERFACE (in.)

the CDC 6400 computer of Lehigh University. This increase in the mesh size is not believed to have any important implications as far as accuracy is concerned. The program was run in the specific case of a 4 inch x 4 inch ingot of 308L stainless steel, in order to try to correlate experimental and theoretical results. It was found that the temperature distribution on the center plane of the ingot was very different from the temperature distribution in the two dimensional model. To be more precise, it was found that the metal pool was much shallower, due to the additional cooling on two sides of the ingot. Figure 14 shows the differences in the pool depth between the two dimensional and three dimensional program for several extraction speeds, the same process parameters being used in the two programs.

As can be seen from Figure 14, the linear relationship between the pool depth and the extraction speed is still valid in the three dimensional analysis. However, the pool depth increases much more slowly when the melting rate increases.

CORRELATION BETWEEN EXPERIMENTAL AND THEORETICAL RESULTS

The correct pool depths could not be predicted accurately by using a constant temperature distribution across the ingot section at the slag metal interface. A parabolic profile was assumed, using a temperature of 2800°F at the center of the ingot section and a temperature of 2700°F at the center of the ingot faces. The assumed temperature distribution at the top of the ingot is therefore a paraboloid of revolution. A heat transfer coefficient of 60 $Btu/ft^2/Hr/°F$ was chosen for representing the heat transfer between the mold and the ingot when the temperature of the metal is above the solidus temperature. A heat transfer coefficient of 30 $Btu/ft^2/Hr/°F$ was assumed in the lower part of the mold. In the sprayed zone, a heat transfer coefficient of 300 $Btu/ft^2/Hr/°F$ was assumed. (A higher heat transfer coefficient has not been found to influence the shape of the pool for a 4 inch mold, although it does decrease the temperature in the lower part of the ingot.) A conductivity of 20 $Btu/ft^2/Hr/°F$ was assumed for

Figure 14

Comparison of the relationship between pool depth and speed of extraction obtained with the two-dimensional and the three-dimensional program.

4

THE SAME PARAMETERS HAVE BEEN USED IN THE TWO AND THREE DIMENSIONAL ANALYSIS.

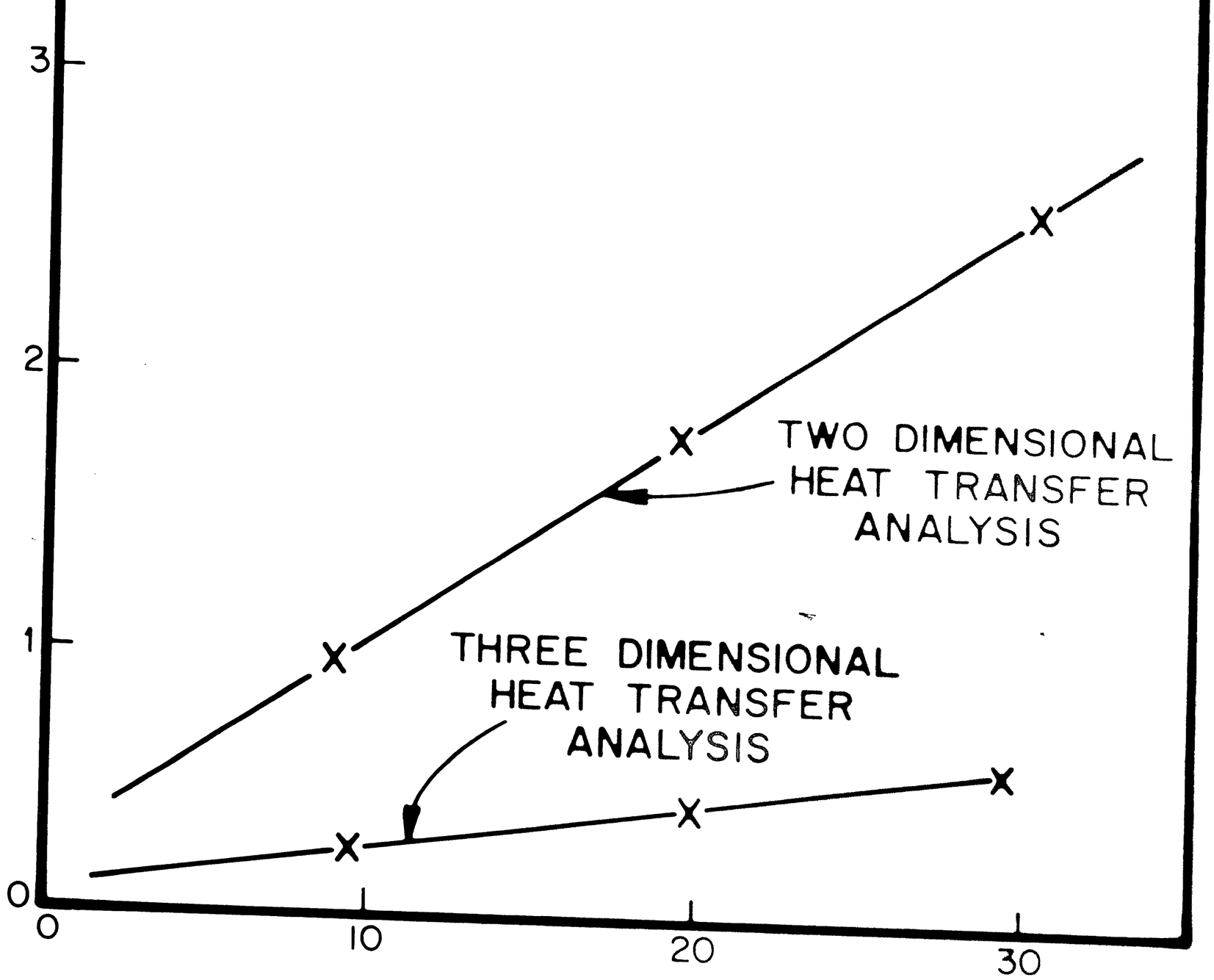

the liquid metal, which corresponds to a certain degree of stirring in the liquid pool. Figures 15 to 18 show the shapes of some isotherms in horizontal and vertical section of the ingot for several extraction speeds. Figure 19 shows the dependence of the depth of the metal pool with the melting rate for the process parameters selected as discussed earlier and the experimental results. Figures 20 and 21 show the agreement between experimental and theoretical results for longitudinal and transverse sections of the ingot, in the case of experimental run number 2.

As can be seen on Figure 6, the first experimental run gave a slightly bell shaped pool. This shape was believed to be due to a "better than usual" heat transfer coefficient between the ingot and the mold. Indeed the exact shape can be obtained by the computer model by using a higher heat transfer coefficient in the upper part of the mold. A heat transfer of 80 $Btu/ft^2/Hr/^\circ F$ was found to give the correct shape. Figure 22 shows the agreement between the experimental and the theoretical curve. A sensitivity study was performed with three different heat transfer coefficients to find the corresponding shape of the molten metal pool. Its result is summarized on Figure 23. It can be seen that a better heat transfer between ingot and mold does not affect very much the depth of the pool but changes its shape.

In view of Figures 19, 20, 21 and 22, it can be seen that the model predicts rather accurately the shape of the molten metal pool for the experimental results available. A closer fitting of experimental and theoretical results could be done, by selecting slightly different temperature at the slag metal interface. This adjustment, however, would not have much significance since a larger number of experimental points would have been necessary to get a feeling about the dependence of the metal pool depth on the melting rate.

It is believed that more complete experimental study of the process on a wider range of melting rates would not give a linear relationship

Figure 15

Isotherms in a transverse section of the ingot 0.3 inch below slag-metal interface.

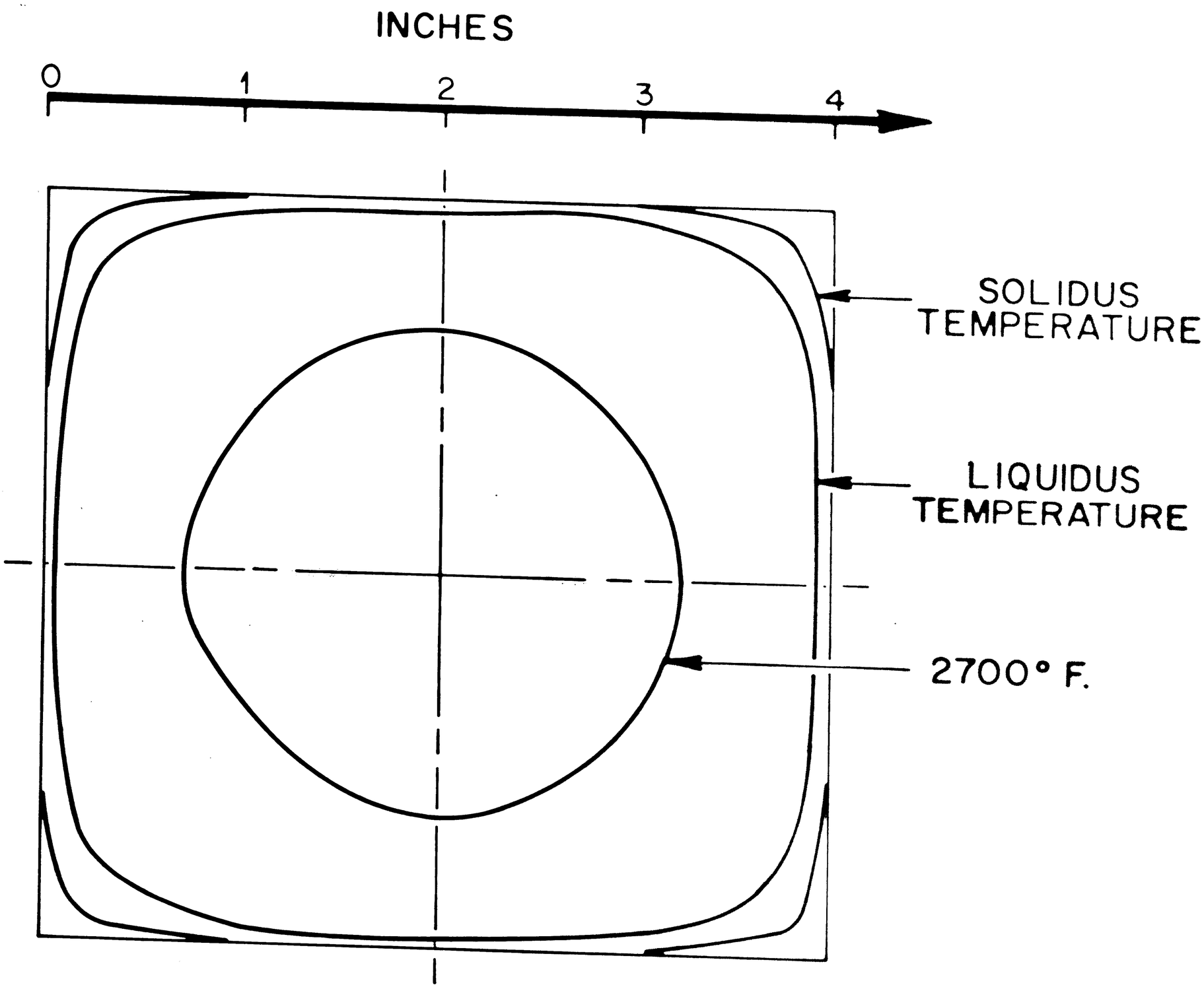

—— ISOTHERM

TRANSVERSE SECTION OF THE INGOT 0.3 in. BELOW SLAG METAL INTERFACE.

MELTING RATE = 30 in./hr

Figure 16

Isotherms in a transverse section of the ingot 0.75 inch below slag-metal interface.

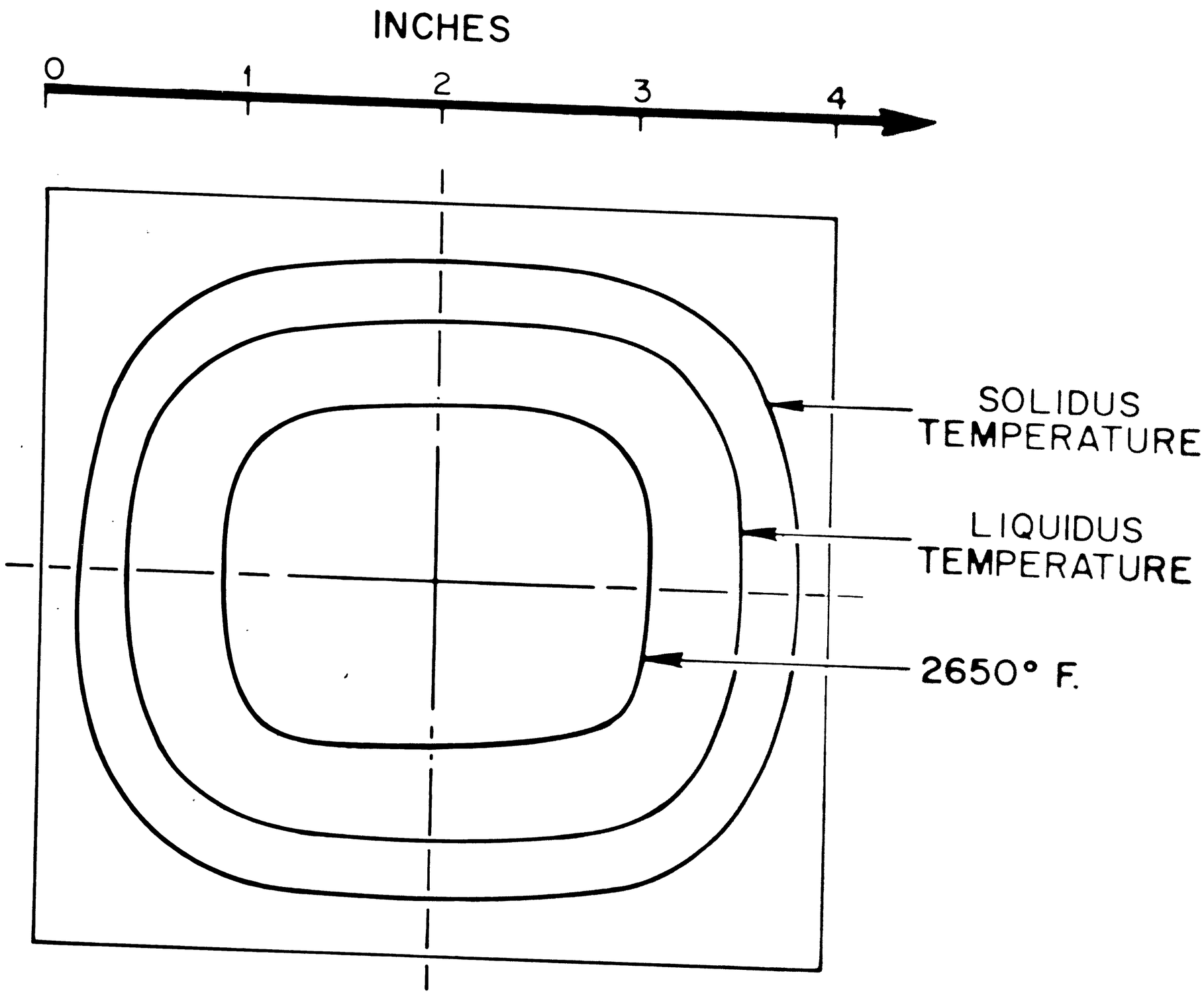

—— ISOTHERM

TRANSVERSE SECTION OF THE INGOT 0.75 in. BELOW SURFACE.

MELTING RATE = 10 in./hr

Figure 17

Isotherms in a longitudinal section of the ingot for three different extraction speeds.

Process parameters:

extraction speed: 10, 20, 30 inches per hour

heat transfer coefficient in the mold { 50 Btu/ft^2/Hr/°F for T > 2550°F
30 Btu/ft^2/Hr/°F for T < 2550°F

heat transfer coefficient in the sprayed zone: 300 Btu/ft^2/Hr/°F

grade of steel: 308L stainless

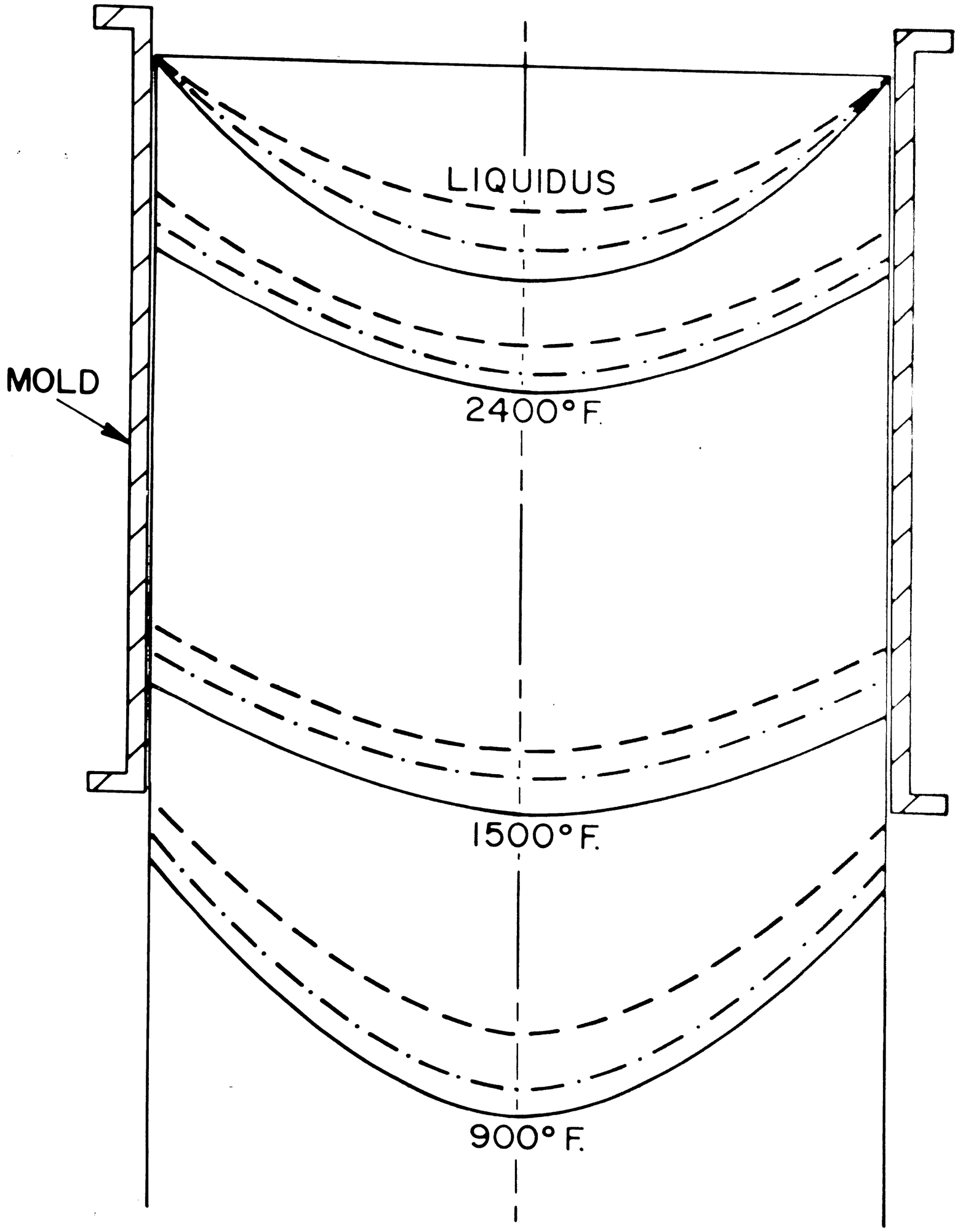

SPEED OF EXTRACTION

— — — 10 in./hr

—·—· 20 in./hr

——— 30 in./hr

Figure 18

Temperature profiles along the centerline and on the surface of the ingot (in a plane of symmetry) for several speeds of extraction.

Curves No. 1 Temperature profile along the centerline of one face of the ingot.

Curves No. 2 Temperature profile along the centerline of the ingot.

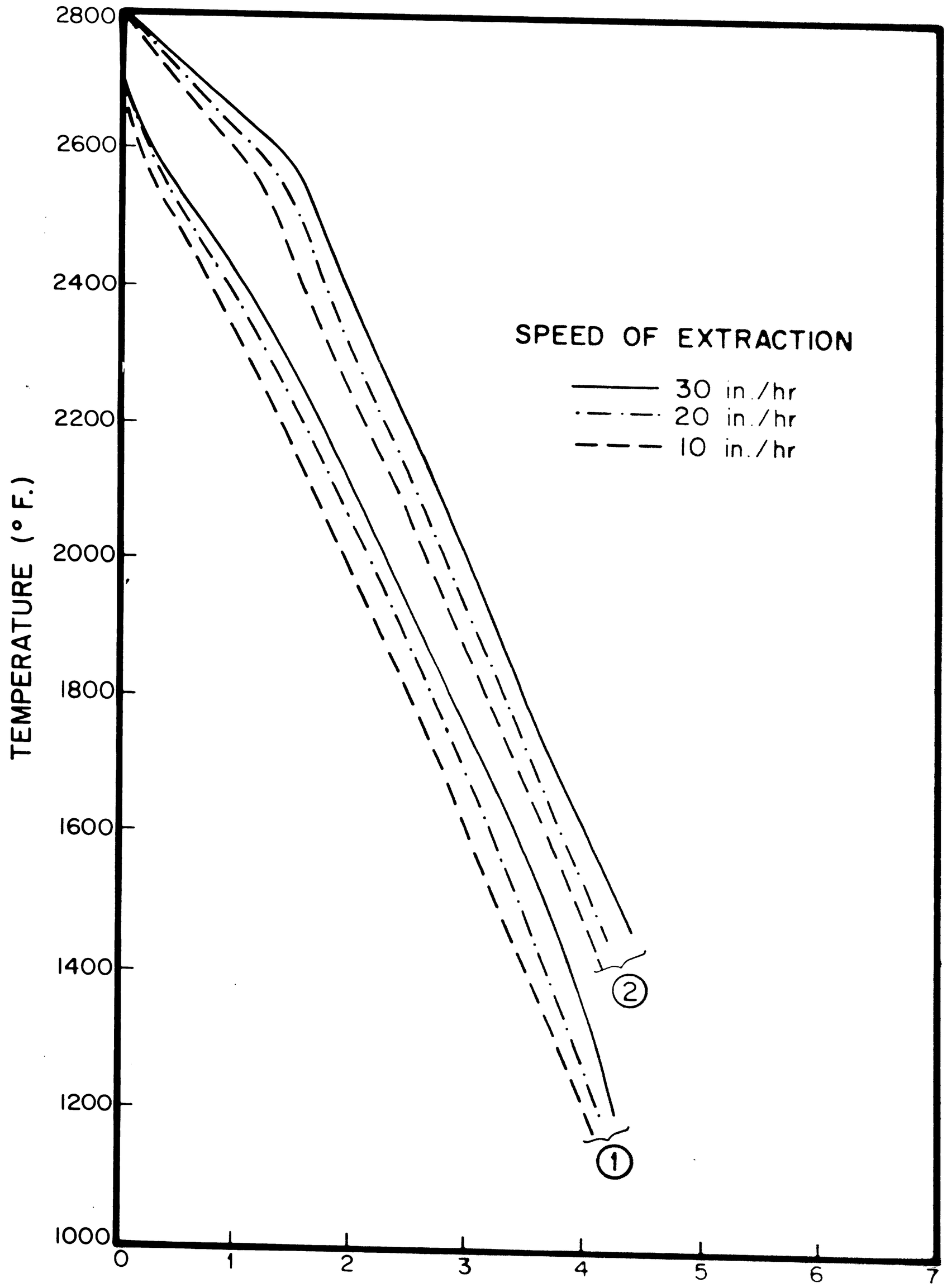
SPEED OF EXTRACTION
30 in./hr
20 in./hr
10 in./hr
TEMPERATURE (° F.)
2800
2600
2400
2200
2000
1800
1600
1400
1200
1000
0
1
2
3
4
5
6
7
①
②
DISTANCE FROM THE SLAG METAL INTERFACE (in.)

Figure 19

Relationship between pool depth and extraction speed. Correlation between experimental and theoretical results.

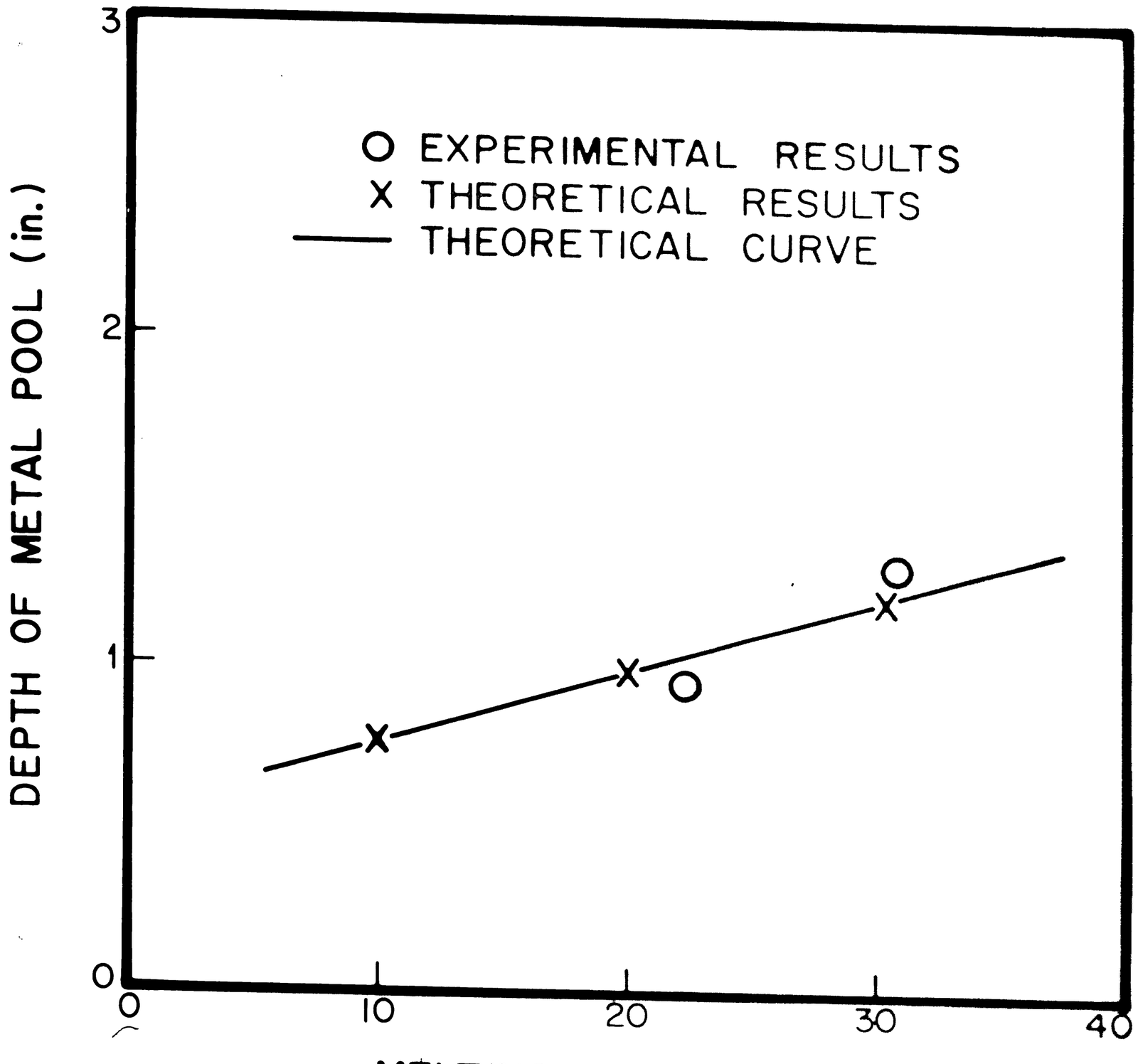
O EXPERIMENTAL RESULTS
X THEORETICAL RESULTS
THEORETICAL CURVE
DEPTH OF METAL POOL (in.)
0
1
2
0
10
20
30
40
MELTING RATE (in./hr)

Figure 20

Pool shape: Correlation between experimental and theoretical results.
Longitudinal section of the ingot.

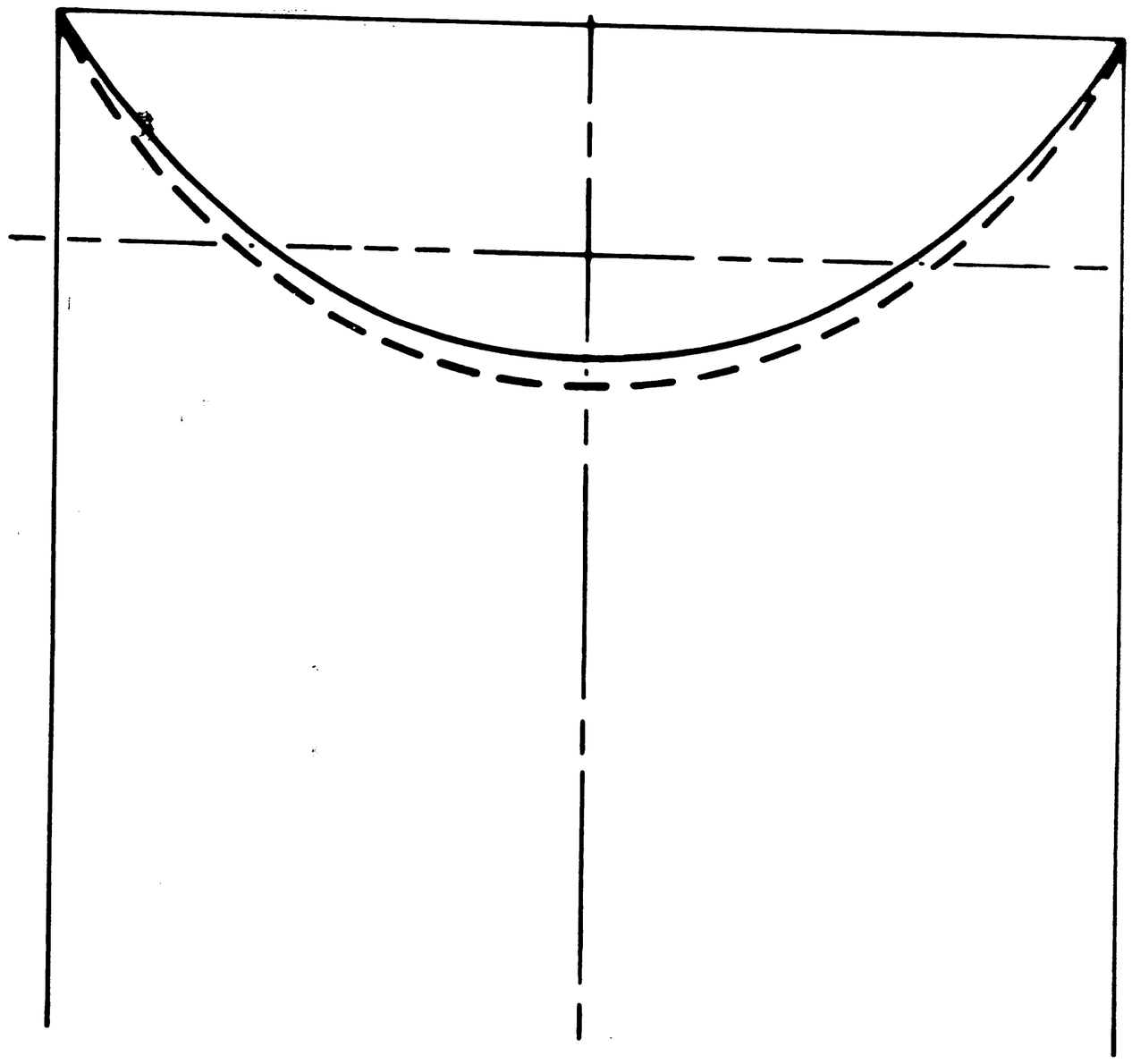

——— COMPUTER RESULT
— — — EXPERIMENTAL RESULT

MELTING RATE = 30 in./hr
THE EXPERIMENTAL CURVE CORRESPONDS TO EXPERIMENT NO. 2 .

Figure 21

Pool shape: Correlation between experimental and theoretical results.
Transverse section of the ingot.

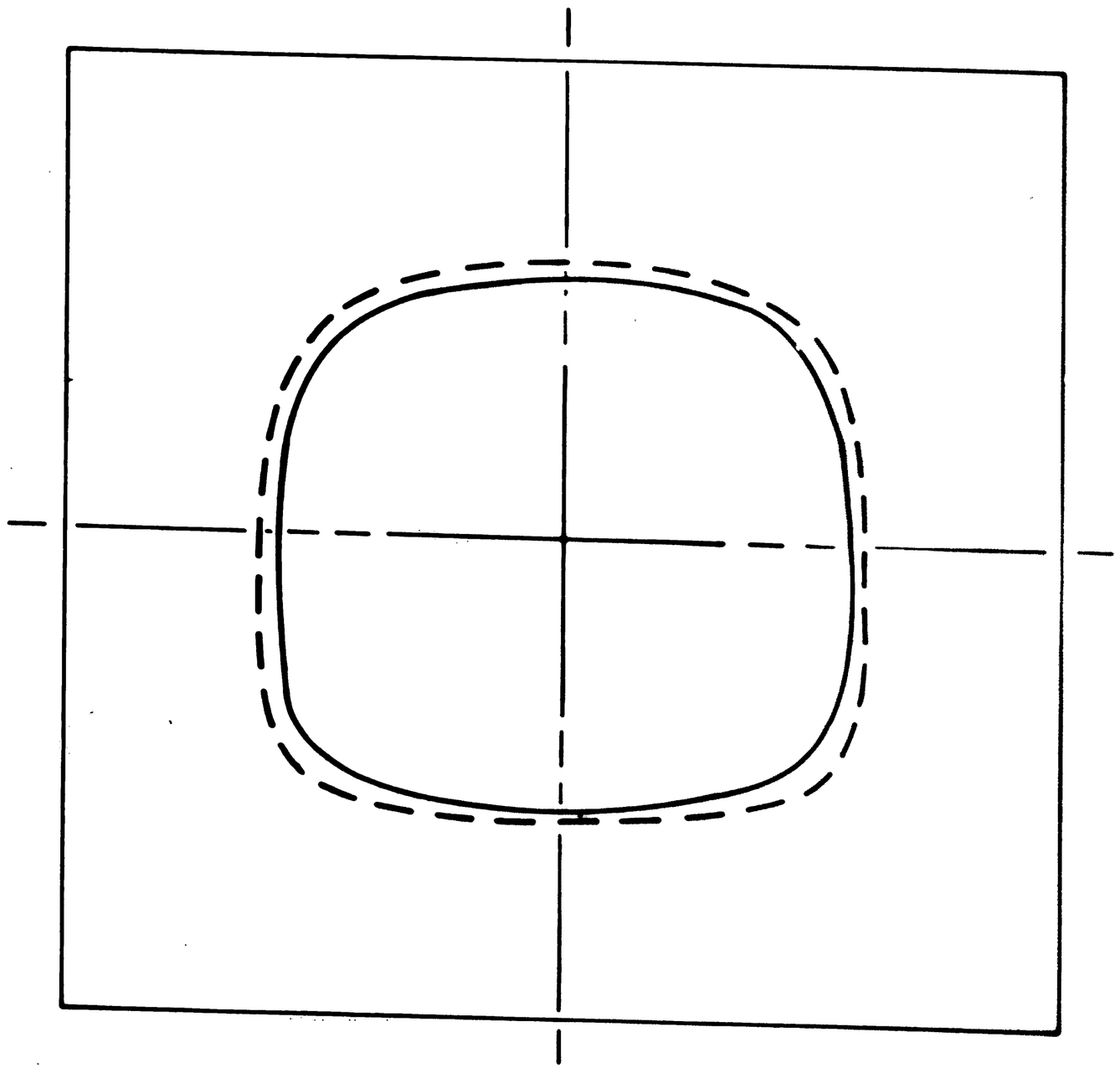

——— COMPUTER RESULT
– – – EXPERIMENTAL RESULT

MELTING RATE = 30 in./hr

THE EXPERIMENTAL CURVE CORRESPONDS TO EXPERIMENT NO. 2 .

Figure 22

Correlation between experimental and theoretical results. Experimental run No. 1.

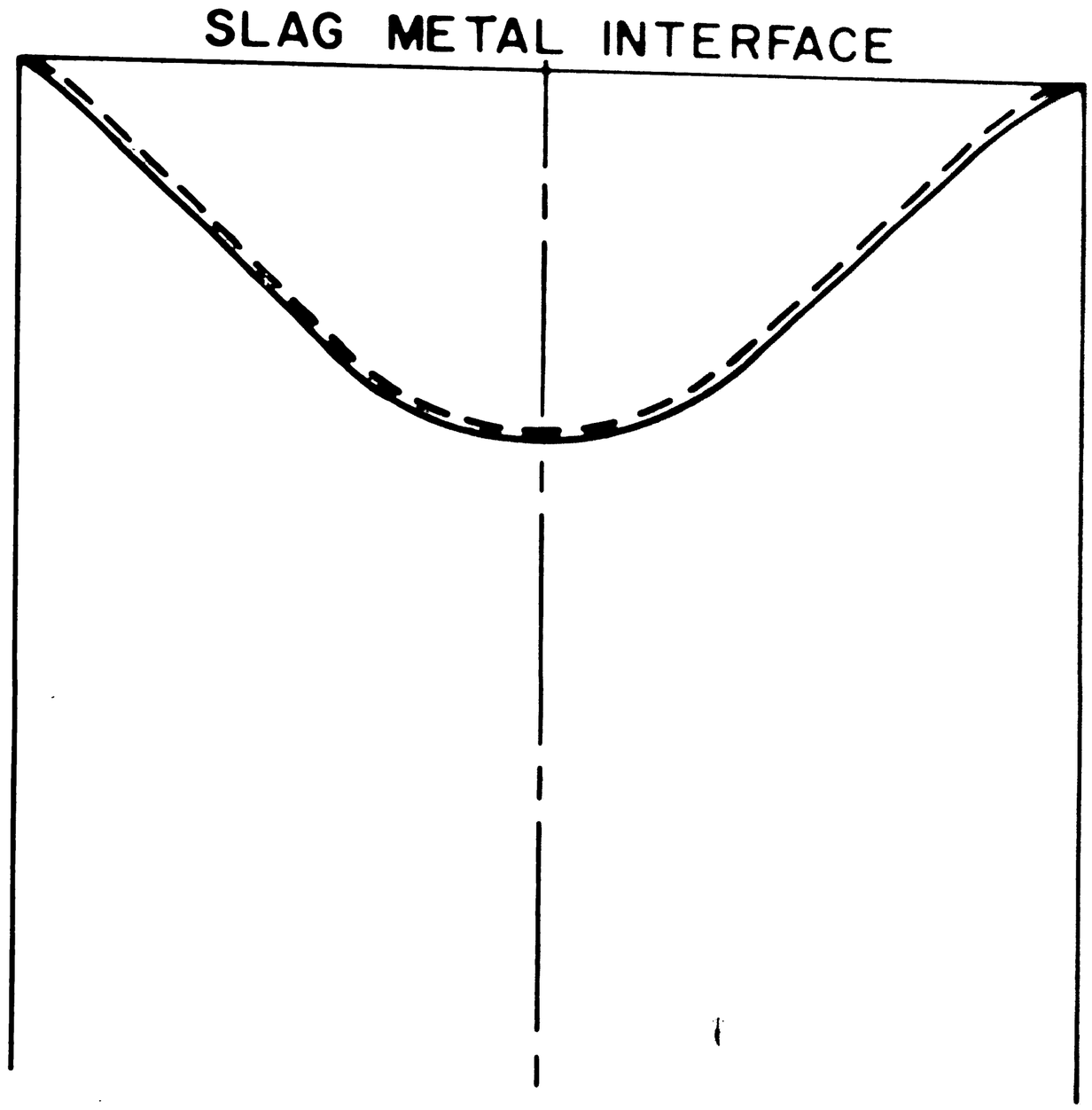

——— COMPUTER RESULT
— — — EXPERIMENTAL RESULT

HEAT TRANSFER COEFFICIENT IN THE UPPER PART OF THE MOLD -
80 Btu/ft^2/hr/°F.

Figure 23

Shape of the molten metal pool for different heat transfer coefficients in the mold.

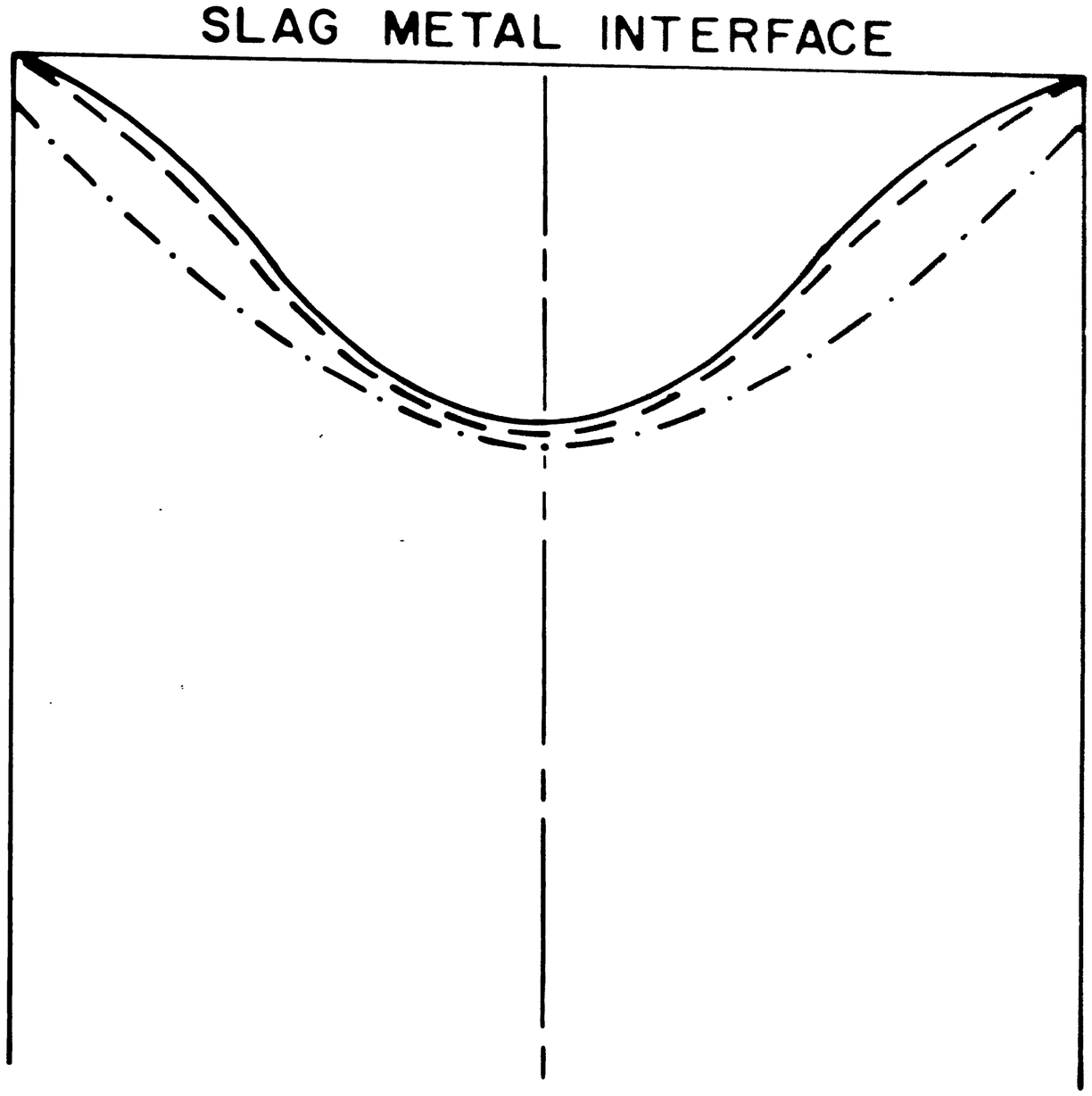

HEAT TRANSFER COEFFICIENT IN THE UPPER PART OF THE MOLD

·—·—· 30 Btu/ft^2/hr/°F.

— — — 80 Btu/ft^2/hr/°F.

——— 150 Btu/ft^2/hr/°F.

as given by the model. The reason is that a change in the melting rate induces a change in the amount of superheat of the droplets so that the boundary condition at the slag-metal interface varies for each melting rate.

In future studies of the heat transfer process in the electro-slag remelting process, attention should be brought to an understanding of the true heat transfer process at the slag-metal interface and to the dependence of the droplets superheat on the melting rate.

CONCLUSION

A mathematical model of the solidification of an electroslag remelted ingot has been developed which predicts the temperature distribution in the remelted ingot and the shape of the molten metal pool. A two dimensional simulation gave some understanding of the process and some qualitative results. A three dimensional simulation then gave results which exhibit a good correlation with experimental results.

The increase in the melting rate seems to contribute in a major part to the increase in the metal pool depth. Future studies should determine if the surface temperature at the slag metal interface is also affected by the melting rate.

The three dimensional heat transfer analysis proposed in this investigation is generalizable in practice to a slab of any dimensions or even more complicated shapes involving square or rectangular subregions.

NOMENCLATURE

C_p	Specific Heat (Btu/Lb/°F)
h	Heat Transfer Coefficient (Btu/ft^2/Hr/°F)
K	Thermal Conductivity (Btu/in/Hr/°F)
L_H	Latent Heat of Fusion (Btu/Lb)
$\overline{\overline{M}}$	Matrix of the Coefficients of the Finite Difference Equation
Q	Heat Generation Term (Btu/Hr/inches^2)
ρ	Density (Lb/inches^3)
Δt	Time Step (hour)
T	Temperature (°F)
T_{sol}	Solidus Temperature (°F)
T_{liq}	Liquidus Temperature (°F)
V	Melting Rate (or Extraction Speed) (inches/h)

APPENDIX I

Derivation of S.I.P. Algorithm

For purpose of generality, the S.I.P. algorithm will be derived here for a three dimensional problem. The two dimensional S.I.P. algorithm is simply obtained by cancelling the terms referring to the additional dimension. The details of the matrix multiplication and the proof of convergence of the algorithm are not included in this derivation. More details about the procedure can be found in the two papers published on the subject(1,2).

If the nodes (i, j, k) are ordered in sequence such that i is swept through first (i = 1, 2, --- I), j second (j = 1, 2 --- J) and k last (k = 1, 2 --- K), the temperatures T_{ijk} at the nodes can be arranged in a vector $\vec{T}$.

Considering now the difference equation derived in Appendix II:

$$Z_{i,j,k}\, T_{i,j,k-1} + B_{i,j,k}\, T_{i,j-1,k} + D_{i,j,k}\, T_{i-1,j,k} + E_{i,j,k}\, T_{i,j,k}$$

$$+ F_{i,j,k}\, T_{i+1,j,k} + H_{i,j,k}\, T_{i,j+1,k} + S_{i,j,k}\, T_{i,j,k+1} = q_{i,j,k}$$

and ordering this equation in the same sequence, the overall system can be written:

$$\overline{\overline{M}}\ \overline{T} = \overline{q} \qquad (1)$$

$\overline{\overline{M}}$ being a (I x J x K) x (I x J x K) matrix.(Figure 24) A direct solution of (1) would be very time consuming, although the matrix M is very sparse.

The essence of the algorithm is to add to the matrix M a matrix N so that (M + N) is factorable into a lower triangular matrix L and an upper triangular matrix U, which are also sparse.[1]

---

[1] Any matrix is factorable into an upper and lower triangular matrices, but in this algorithm, U and L must satisfy some a priori requirements.

Figure 24

Matrix formulation of the finite difference scheme.

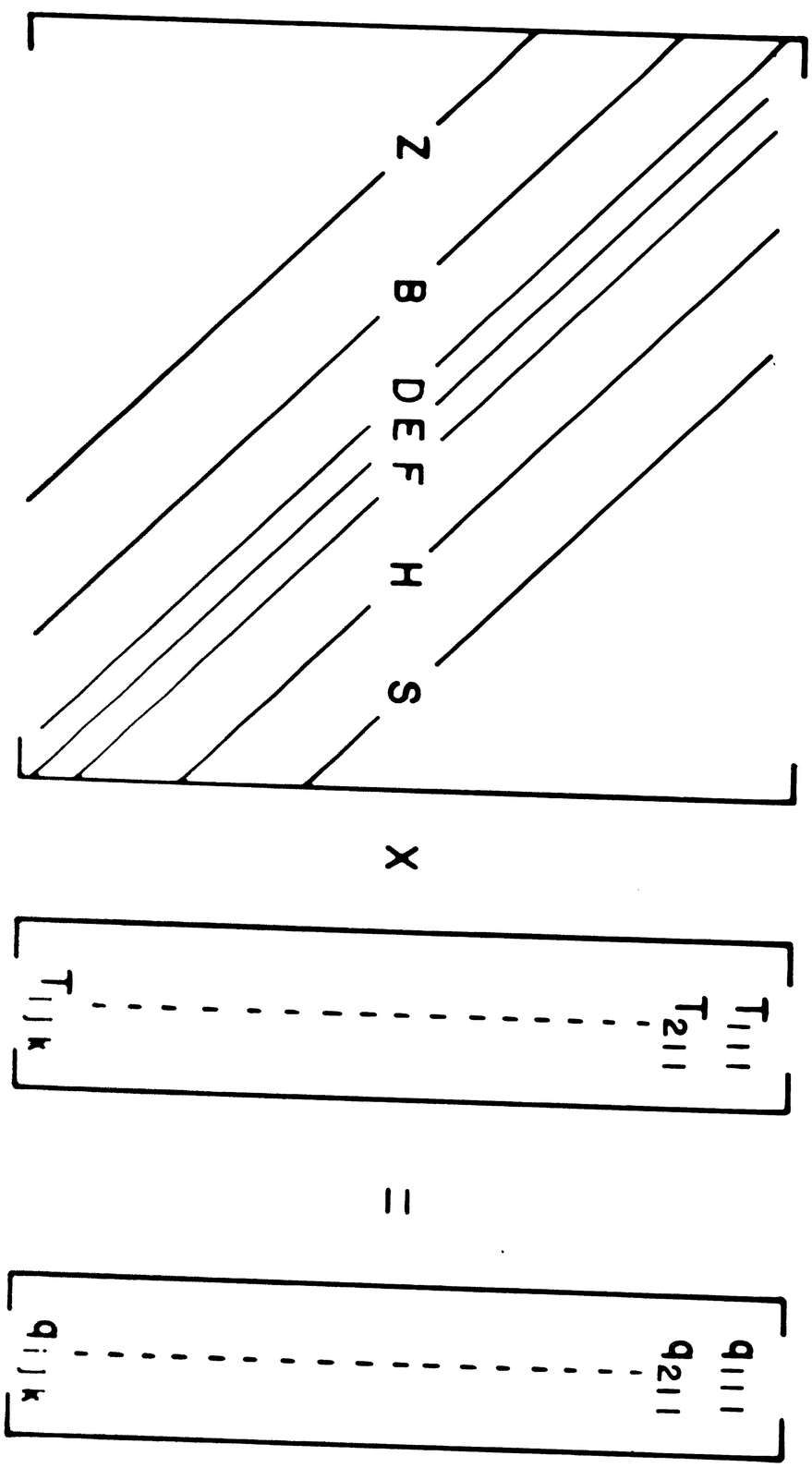
Z
B
DEF
H
S
X
T_{111}
T_{211}
T_{ijk}
=
q_{111}
q_{211}
q_{ijk}

Equation 1 becomes:

$$(M + N)\ T = q + NT.$$

The iteration scheme is then the following:

$$(M + N)\ T^{n+1} = q + NT^{n}$$ (The superscripts denote the iteration level)

or:

$$(M + N)\ T^{n+1} = q + NT^{n} + MT^{n} - MT^{n}$$

$$(M + N)\ (T^{n+1} - T^{n}) = q - MT^{n}$$

Defining $R^{n} = q - MT^{n}$

$$(M + N)\ \Delta T^{n+1} = R^{n}$$

Since $(M + N) = LV$, the algorithm is defined by $LU\Delta T^{n+1} = R^{n}$

Defining $V = U\Delta T^{n+1}$, the following expression is obtained $LV = R^{n}$

U and V being sparse, triangular matrices, they can be easily inverted, and the iteration proceeds in the following way:

$$R^{n} = q - MT^{n}$$

$$V = L^{-1}R^{n}$$

$$\Delta T^{n+1} = U^{-1}V$$

The actual equations of the S.I.P. algorithms are not reproduced here. For more information, see Reference 1 and 2 and the listing of the computer program. A flow chart of the algorithm is given in Figure 25.

Figure 25

S.I.P. algorithm flow chart.

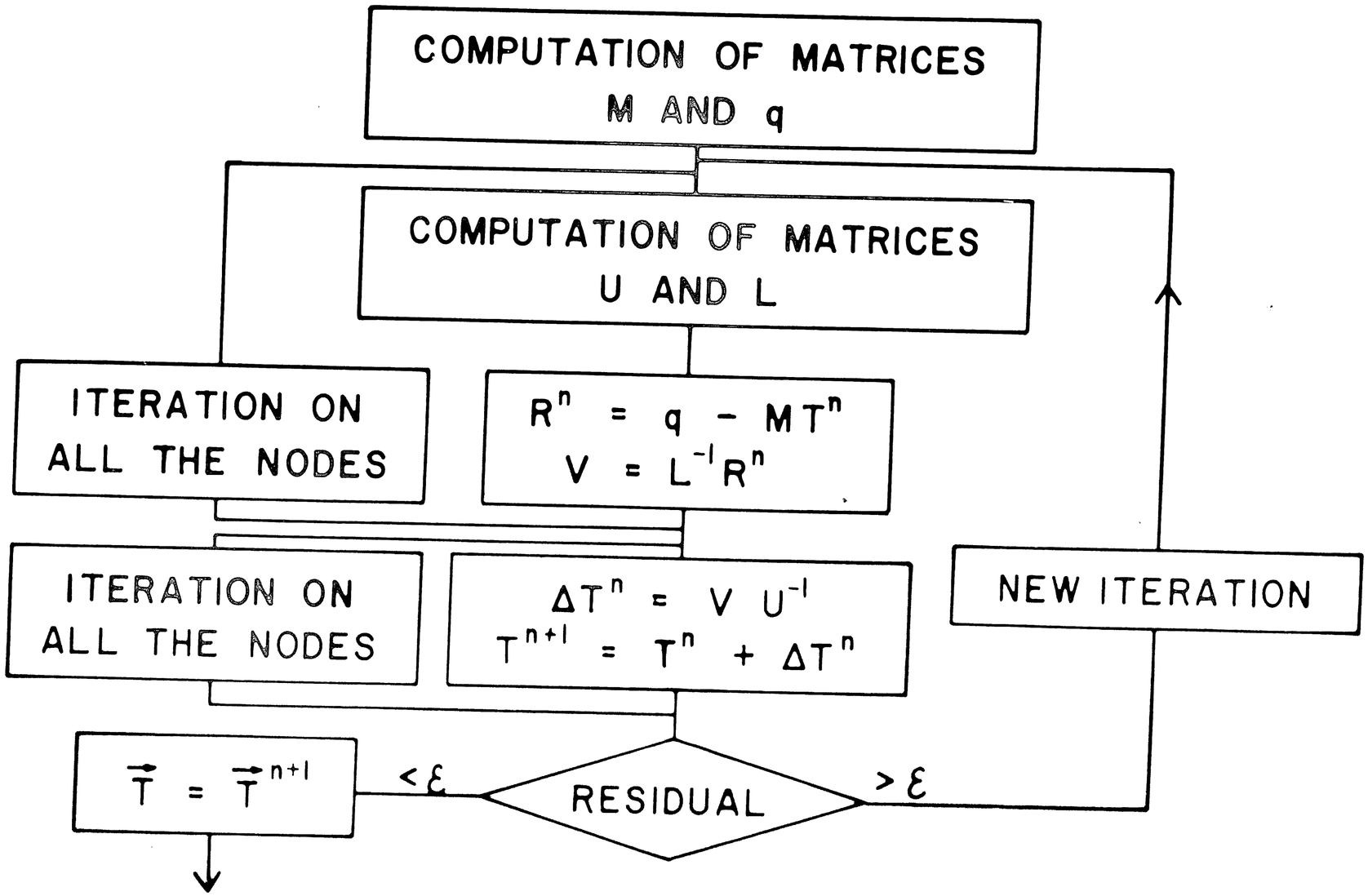
COMPUTATION OF MATRICES
M AND q
COMPUTATION OF MATRICES
U AND L
ITERATION ON
ALL THE NODES
$R^n = q - MT^n$
$V = L^{-1}R^n$
ITERATION ON
ALL THE NODES
$\Delta T^n = V U^{-1}$
$T^{n+1} = T^n + \Delta T^n$
NEW ITERATION
$\vec{T} = \vec{T}^{n+1}$
$< \varepsilon$
RESIDUAL
$> \varepsilon$

APPENDIX II

Derivation of the Finite Difference Scheme in Three Dimensions

A. Unsteady State

1. Constant mesh size:

The partial differential equation can be written:

$$\frac{\partial}{\partial x}\left(K\frac{\partial T}{\partial x}\right)+\frac{\partial}{\partial y}\left(K\frac{\partial T}{\partial y}\right)+\frac{\partial}{\partial z}\left(K\frac{\partial T}{\partial z}\right)=\rho C_p\frac{\partial T}{\partial t}+Q$$

By Taylor series expansion of the function T around the node (i, j, k) corresponding to the value x_i, y_j, z_k of the coordinates, the term $\frac{\partial}{\partial x}\left(K\frac{\partial T}{\partial x}\right)$ can be approximated by

$$K_{i+\frac{1}{2},j,k}\frac{(T_{i+1,j,k}-T_{i,j,k})}{\Delta x^2}-K_{i-\frac{1}{2},j,k}\frac{(T_{i,j,k}-T_{i-1,j,k})}{\Delta x^2}$$

Similar expressions are obtained for $\frac{\partial}{\partial y}\left(K\frac{\partial T}{\partial y}\right)$ and for $\frac{\partial}{\partial z}\left(K\frac{\partial T}{\partial z}\right)$; the finite difference form of the partial differential equation then takes the following form:

$$Z_{i,j,k}T^n_{i,j,k-1}+B_{i,j,k}T^n_{i,j-1,k}+D_{i,j,k}T^n_{i-1,j,k}+E_{i,j,k}T^n_{i,j,k}$$

$$+F_{i,j,k}T^n_{i+1,j,k}+H_{i,j,k}T^n_{i,j+1,k}+S_{i,j,k}T^n_{i,j,k+1}=q_{i,j,k}$$

where $B_{i,j,k}=K_{i,j-\frac{1}{2},k}\frac{\Delta x\Delta z}{\Delta y}$

$$q_{i,j,k}=\left[Q_{i,j,k}-\frac{1}{\Delta t}\rho_{i,j,k}C_{p_{i,j,k}}T^{n-1}_{i,j,k}\right]\Delta x\Delta y$$

The superscript n in $T^n_{i,j,k}$ denotes the value of $T_{i,j,k}$ at the n^{th} time interval.

2. Variable mesh size:

In the case of a variable mesh size, similar to the drawing of Figure 26, the finite difference form of the expression $\frac{\partial}{\partial x}\left(K \frac{\partial T}{\partial x}\right)$ can be written:

$$K_{i+\frac{1}{2},j,k} \frac{2(T_{i+1,j,k} - T_{i,j,k})}{\Delta x_a (\Delta x_a + \Delta x_b)} - K_{i-\frac{1}{2},j,k} \frac{2(T_{i,j,k} - T_{i-1,j,k})}{\Delta x_b (\Delta x_a + \Delta x_b)}$$

The value of the coefficients in the finite difference equation are as follows:

$$B_{i,j,k} = K_{i,j-\frac{1}{2},k} \frac{(\Delta x_a + \Delta x_b)(\Delta z_a + \Delta z_b)}{4\Delta y_b}$$

$$D_{i,j,k} = K_{i-\frac{1}{2},j,k} \frac{(\Delta y_a + \Delta y_b)(\Delta z_a + \Delta z_b)}{4\Delta x_b} \quad \text{------ etc.}$$

To check the validity of the derivation of the finite difference equation in the case of variable mesh size, it is convenient to consider the equation as a heat balance around the (i, j, k) node.

B. Steady State

The steady state equation, written by reference to a fixed coordinate system with respect to which the ingot is moving with a velocity V, can be derived by considering a heat balance in an elementary cube of dimensions Δx, Δy and Δz. The rate of accumulation of heat in this cube, due to conduction is $\left[\frac{\partial}{\partial x}\left(K \frac{\partial T}{\partial x}\right) + \frac{\partial}{\partial y}\left(K \frac{\partial T}{\partial y}\right) + \frac{\partial}{\partial z}\left(K \frac{\partial T}{\partial z}\right) \right] \Delta x \Delta y \Delta z$. Since the conditions are steady state, this quantity must be equated to the difference between the amount of heat leaving and entering the cube because of its relative movement with respect to the coordinate system. This quantity is:

$$V \Delta x \Delta y \rho C_p dT + Q \Delta x \Delta y \Delta z.$$

The steady state equation is therefore:

$$\frac{\partial}{\partial x}\left(K \frac{\partial T}{\partial x}\right) + \frac{\partial}{\partial y}\left(K \frac{\partial T}{\partial y}\right) + \frac{\partial}{\partial z}\left(K \frac{\partial T}{\partial z}\right) = \rho C_p V \frac{\partial T}{\partial y} + Q$$

Figure 26

Details on nodes arrangements for variable mesh size.

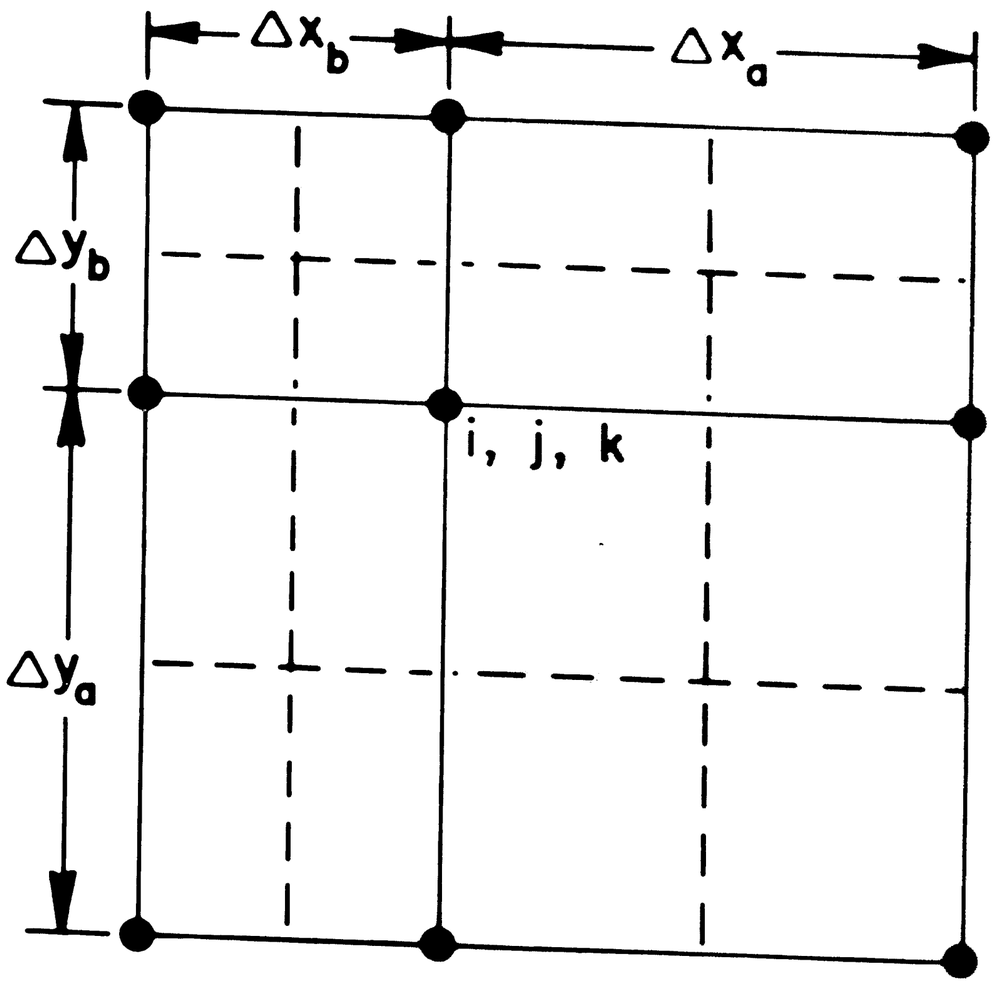

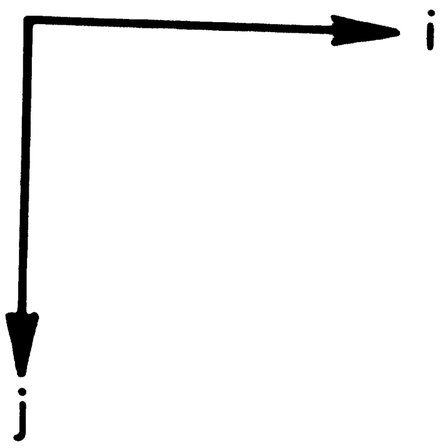

Δx_a, Δx_b = VALUES OF LOCAL MESH SIZE IN THE x DIRECTION.

Δy_a, Δy_b = VALUES OF LOCAL MESH SIZE IN THE y DIRECTION.

This equation is very similar to the unsteady state equation, except that the temperature T is now only a function of the three space variables. The only coefficients affected by the bulk flow term are those related to $T_{i,j-1,k}$ and $T_{i,j,k}$.

The value of $B_{i,j,k}$ is then:

$$B_{i,j,k} = K_{i,j-\frac{1}{2},k} \frac{\Delta x \Delta z}{\Delta y} + V\rho Cp\Delta x\Delta z$$

In the case of variable mesh size:

$$B_{i,j,k} = K_{i,j-\frac{1}{2},k} \frac{(\Delta x_a + \Delta x_b)(\Delta z_a + \Delta z_b)}{4\Delta y_b} + V\rho Cp \frac{(\Delta x_a + \Delta x_b)(\Delta z_a + \Delta z_b)}{4}$$

APPENDIX III

Physical Properties of 308L Stainless Steel

The physical properties of steel at elevated temperatures are not very well established. The best values available in the literature have been selected and are shown in the next figures. Since 308L is not an extremely common steel, some data available for similar stainless steels like 304 and 18.8 have also been used.

The melting range has been selected as 2550°F to 2600°F. The heat of fusion was chosen as 122 Btu/Lb(20).

Figure 27

Variation of specific heat with temperature for 308L.

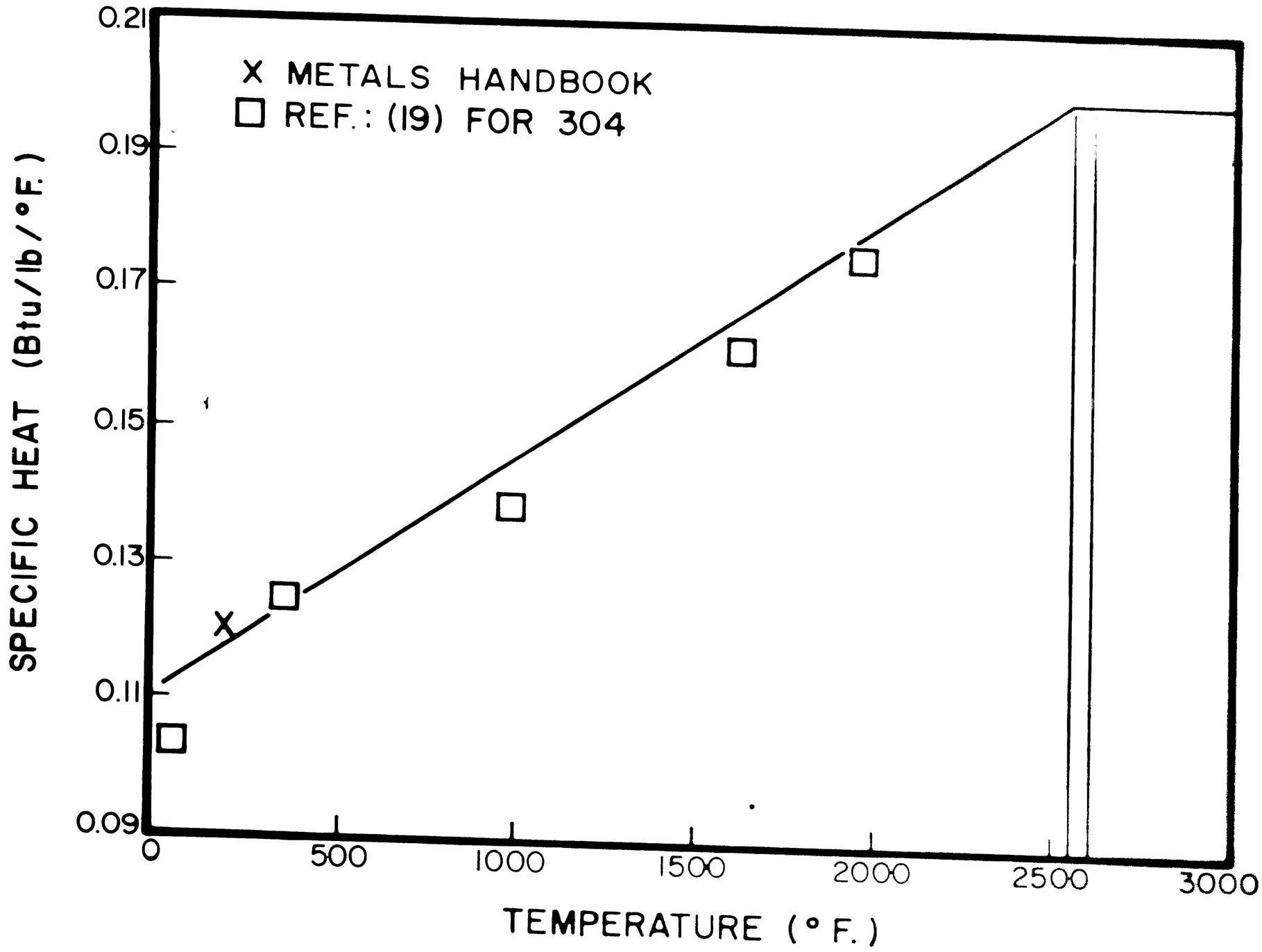
X METALS HANDBOOK
□ REF.: (19) FOR 304
SPECIFIC HEAT (Btu/lb/°F.)
0.21
0.19
0.17
0.15
0.13
0.11
0.09
0
500
1000
1500
2000
2500
3000
TEMPERATURE (° F.)

Figure 28

Variation of density with temperature for 308L.
(The change of density with temperature was computed by using the coefficient of thermal expansion and some general information concerning the density change of steel between the solid and the liquid state.)

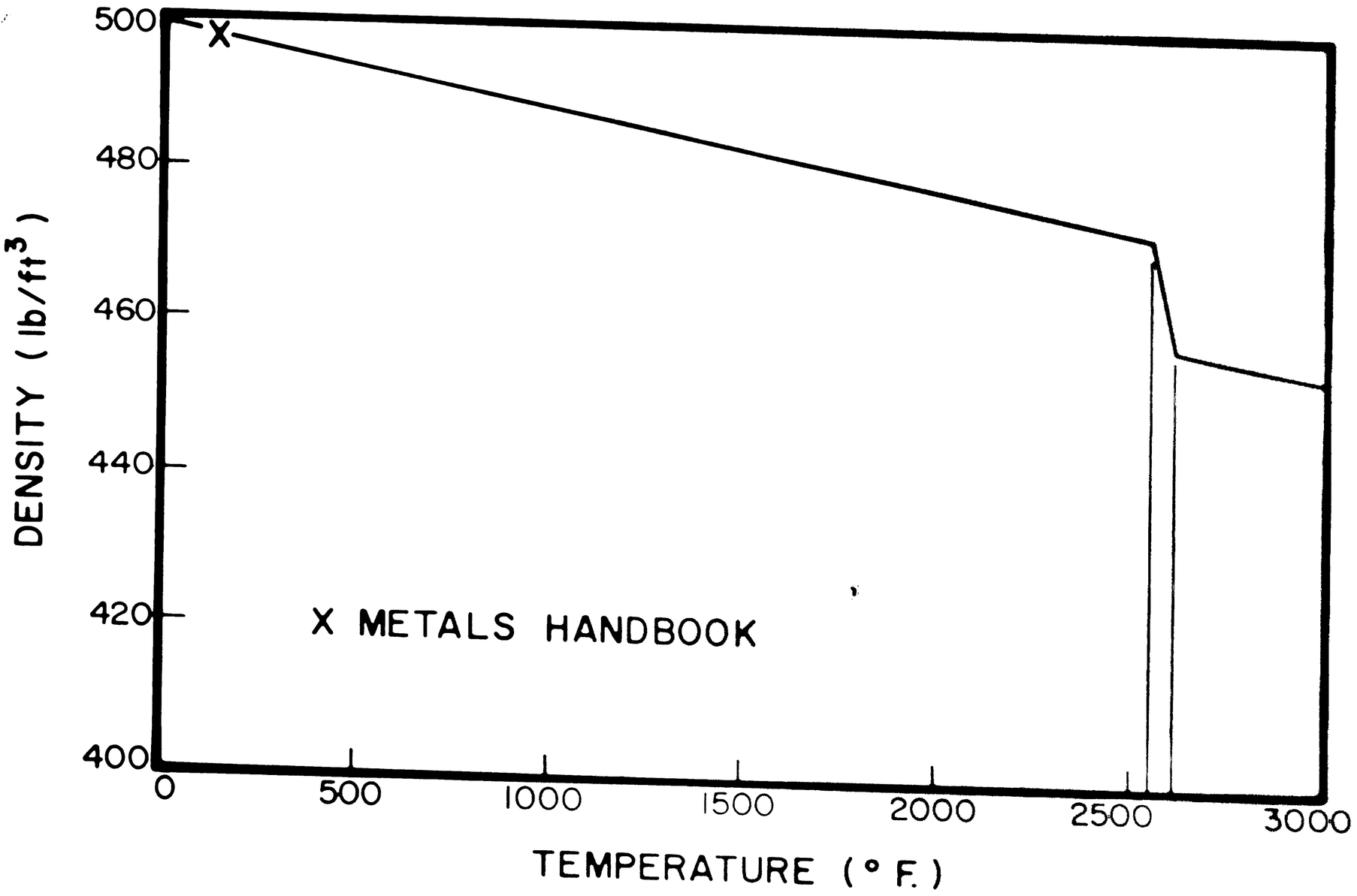
500
480
460
440
420
400
DENSITY (lb/ft3)
X
X METALS HANDBOOK
0
500
1000
1500
2000
2500
3000
TEMPERATURE (° F.)

Figure 29

Variation of thermal conductivity with temperature for 308L.

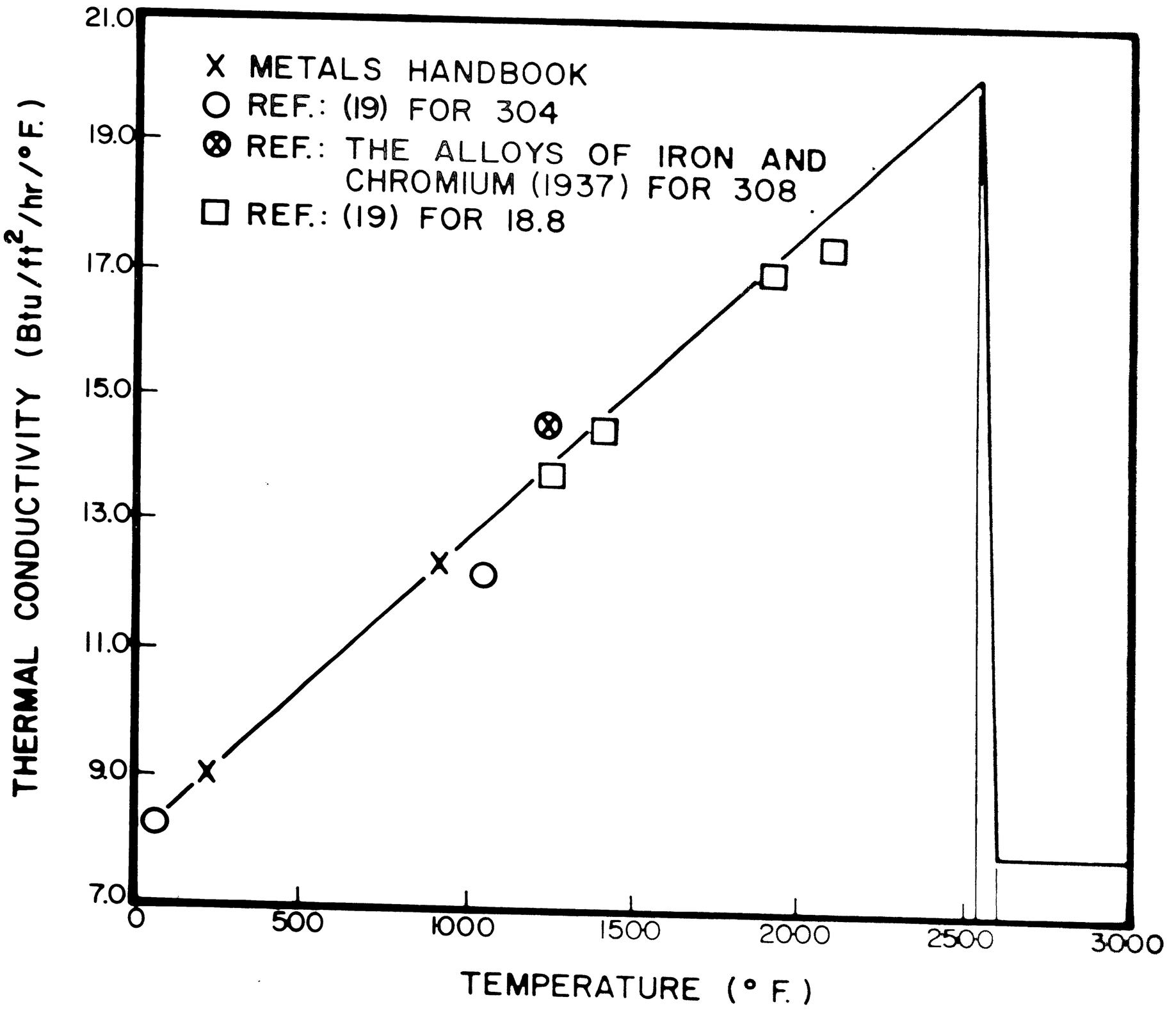
X METALS HANDBOOK
O REF.: (19) FOR 304
⊗ REF.: THE ALLOYS OF IRON AND CHROMIUM (1937) FOR 308
□ REF.: (19) FOR 18.8
THERMAL CONDUCTIVITY (Btu/ft²/hr/°F.)
21.0
19.0
17.0
15.0
13.0
11.0
9.0
7.0
0
500
1000
1500
2000
2500
3000
TEMPERATURE (° F.)

BIBLIOGRAPHY

1. W. C. Winegard, "An Introduction to the Solidification of Metals", The Institute of Metals, London, 1964.

2. A. W. D. Hills, "Simplified Theoretical Treatment for the Transfer of Heat in Continuous-Casting Machine Moulds", J.I.S.I., January 1965, pages 18-26.

3. D. L. Schroeder and D. L. Lippitt, "Two-Dimensional Heat Transfer Simulation for Continuous Casting", AIME Annual Meeting, New York, 1968.

4. J. Savage, "A Theory of Heat Transfer and Air Gap Formation in Continuous Casting Molds", J.I.S.I., January 1962, pages 41-47.

5. R. C. Sun and J. W. Pridgeon, Predicting Pool Shapes in a Laboratory Electroslag Remelting Process, paper given at the Second International Symposium on Electroslag Remelting Technology, Pittsburgh, Pennsylvania, September 1969.

6. J. Douglas and T. M. Gallic, "On The Numerical Integration of a Parabolic Differential Equation Subject to a Moving Boundary Condition", Duke Math. Jr., No. 22, 1955, pages 557-571.

7. M. E. Rose, "On the Melting of a Slab", S.I.A.M. J. Appli. Math., Vol. 15, No. 3, May 1967, pages 495-504.

8. L. H. Ehrlich, "A Numerical Method of Solving a Heat Flow Problem with Moving Boundary", Jr. Assoc. Comp. Mach., Vol. 5, 1958, pages 161-176.

9. B. K. Larkin, "Some Finite Difference Methods for Problems in Transient Heat Flow", Chem. Engineering Series, "Heat Transfer", No. 59, Vol. 61, pages 1-10.

10. H. L. Stone, "Interative Solution of Implicit Approximations of Multidimensional Partial Differential Equations", S.I.A.M. J. Num. Anal., Vol. 5, No. 3, September 1968.

11. D. W. Peaceman and H. H. Rachford, "The Numerical Solution of Parabolic and Elliptic Differential Equations", J. Soc. Indust. Appl. Math., Vol. 3, No. 1, March 1955, pages 28-41.

12. H. G. Weinstein, H. L. Stone and T. V. Kwan, "Iterative Procedure for Solution of Systems of Parobolic and Elliptic Equations in Three Dimensions", I & EC Fundamentals, Vol. 8, No. 2, May 1969.

13. J. P. Holman, Heat Transfer, McGraw Hill Book Company, Inc., New York, 1963, page 5.

14. H. T. Hashemi and C. M. Sliepcevich, "A Numerical Method for Solving Two Dimensional Problems of Heat Conduction with Change of Phase", Chem. Eng. Progress Symposium, Series No. 79, Vol. 63, pages 34-41.

15. R. H. Tieu and G. E. Geiger, "A Heat Transfer Analysis of the Solidification of a Binary Eutectic System", Trans. ASME, J. of Heat Transfer, December 1966.

16. D. A. Dudko, I. N. Rublevskii and G. S. T. Belous, Automatic Welding, Vol. 5, 1959, pages 29-37.

17. J. Campbell, "Fluid Flow and Droplet Formation in the Electroslag Remelting Process", J. of Metals, Vol. 22, No. 7, 1970.

18. B. Chalmers, Principles of Solidification, John Wiley & Sons, Inc., New York.

19. "Report on Physical Properties of Metals and Alloys from Cryogenic to Elevated Temperatures", ASTM, Special Technical Publication No. 296, 1961.

20. L. Nemethy, E. Stock and W. B. F. Mackay, "Continuous Casting", AIME, Proceedings of Technical Session of the Iron and Steel Division, Detroit, Michigan, 1961.

VITA

Jean-Louis Galzin was born on June 20, 1947 in Cransac, France. His parents are George Maurice Pierre Galzin and the former Raymonde Emilienne Delmon. In June 1964, he graduated from Lycee Foch, in Rodez. After two years in a preparatory school at the University of Toulouse, he entered the "Ecole des Mines" in Nancy, one of the French "Grandes Ecoles d'Ingenieur". While at this school, he had two short industrial experiences, one with the Department of Metallurgy of the Danish Atomic Energy Commission and another with IRSID (the French Steel Institute of Research). Mostly involved in Applied Mathematics during his third year at this school, he graduated in June 1969 with the degree of "Ingenieur Civil des Mines".